Modelling the influence of vitamin D and probiotic supplementation on the microbiome and immune response

Mathematical Medicine and Biology: A Journal of the IMA (2024) **41**, 304–345
https://doi.org/10.1093/imammb/dqae017
Advance Access publication on 1 October 2024

Modelling the influence of vitamin D and probiotic supplementation on the microbiome and immune response

S.J. Franks*
School of Mathematical Sciences, University of Nottingham, Nottingham NG7 2RD, UK
*Corresponding author: susan.franks@nottingham.ac.uk

J.L. Dunster
School of Mathematical Sciences, University of Nottingham, Nottingham NG7 2RD, UK
Institute for Cardiovascular and Metabolic Research, University of Reading, Reading RG6 6AS, UK

S.R. Carding
Quadram Institute Biosciences, Norwich Research Park, Norwich NR4 7UQ, UK
Norwich Medical School, University East Anglia, Norwich NR4 7TJ, UK

J.M. Lord
Institute of Inflammation and Ageing, University of Birmingham, Birmingham B15 2WB, UK

M. Hewison
Institute of Metabolism and Systems Research, University of Birmingham, Birmingham B15 2TT, UK

P.C. Calder
School of Human Development and Health, Faculty of Medicine, University of Southampton, Southampton SO16 6YD, UK

and

J.R. King
School of Mathematical Sciences, University of Nottingham, Nottingham NG7 2RD, UK

[Received on 9 November 2023; revised on 5 September 2024; accepted on 23 September 2024]

The intestinal microbiota play a critical role in human health and disease, maintaining metabolic and immune/inflammatory health, synthesizing essential vitamins and amino acids and maintaining intestinal barrier integrity. The aim of this paper is to develop a mathematical model to describe the complex interactions between the microbiota, vitamin D/vitamin D receptor (VDR) pathway, epithelial barrier and immune response in order to understand better the effects of supplementation with probiotics and vitamin D. This is motivated by emerging data indicating the beneficial effects of vitamin D and probiotics individually and when combined. We propose a system of ordinary differential equations determining the time evolution of intestinal bacterial populations, concentration of the VDR:1,25$(OH)_2$D complex in epithelial and immune cells, the epithelial barrier and the immune response. The model shows that administration of probiotics and/or vitamin D upregulates the VDR complex, which enhances barrier function and protects against intestinal inflammation. The model also suggests co-supplementation to be superior to individual supplements. We explore the effects of inflammation on the populations of commensal and pathogenic bacteria and the vitamin D/VDR pathway and discuss the value of gathering additional experimental data motivated by the modelling insights.

Keywords: microbiota; vitamin D receptor; inflammation and immune response; supplementation.

1. Introduction

Understanding the complex interactions between the intestinal microbiota, vitamin synthesis, intestinal barrier integrity and the immune response, including its inflammatory component, is crucial for better comprehension of human health and disease (Abboud *et al.,* 2020). Dysbiosis (i.e. an imbalance in microbial composition, changes in microbial metabolism, or changes in microbial distribution throughout the gastrointestinal tract) or adverse changes to the intestinal microbiota composition due to lifestyle and behavioural factors (e.g. medications and antibiotics, adopting a poor diet or changes in geography), damage to the host–microbiota interface, or alterations of the immune system can result in an increased susceptibility to pathogenic invasion and the onset of infectious disease. Such dysregulation can also result in a heightened immune response and chronic inflammation resulting in tissue damage and various diseases e.g. inflammatory bowel disease (IBD), obesity and diabetes (Cristofori *et al.,* 2021).

Manipulation of the intestinal microbiota with dietary components such as prebiotics, probiotics and vitamin D has been shown to contribute to the restoration of normobiosis (Tangestani *et al.,* 2021). Increased vitamin D receptor (VDR) expression by epithelial and immune cells may decrease microbial dysbiosis, enhance barrier function, increase the expression of antimicrobial peptides (AMPs), decrease pro-inflammatory cytokines and increase the production of beneficial short-chain fatty acids (SCFAs) (Abboud *et al.,* 2020; Tangestani *et al.,* 2021; Xong *et al.,* 2020). AMPs (mainly defensins and cathelicidins) are key regulators of interactions between constituents of the microbiota and host tissues and exert a range of antimicrobial activities via sequestering key growth nutrients, permeabilizing bacterial membranes and other related mechanisms, thereby playing an important role in the maintenance of both microbial homeostasis and host defence (Xong *et al.,* 2020). Vitamin D has also been shown to preserve intestinal barrier homeostasis and tight junction complexes in the intestinal epithelium reducing dysbiosis and bacterial colonization (Tangestani *et al.,* 2021).

Likewise, probiotics, which are ingestible health promoting living microorganisms, have also been shown to improve the balance of the intestinal microbiota by regulating its constituents and metabolic output (Vos *et al.,* 2017). Probiotics have been associated with protective effects in the intestine, with some strains regulating immune cells via the interaction of bacterial cell-wall components or secreted bacterial products with immune or epithelial cells in the intestinal mucosa (Vos *et al.,* 2017). Others induce alterations in production of pro-inflammatory and regulatory cytokines (Stojanov *et al.,* 2020) or beneficially contribute to the organization of the epithelial tight junctions via regulation of specific tight junction proteins (e.g. occludin) (Vos *et al.,* 2017; Mujagic *et al.,* 2017).

The beneficial effects of combined supplementation with vitamin D and probiotics in modulating the intestinal microbiota, in addition to fostering healthy microbe–host interactions, are discussed in Abboud *et al.* (2020) and Pagnini *et al.* (2021). This co-supplementation provides a possible therapeutic option for diseases such as IBD. Probiotics have been shown to increase intestinal vitamin D absorption, and to increase VDR protein expression and transcriptional activity (Singh *et al.,* 2020). Likewise, VDR status seems to regulate the mechanisms of action of probiotics and modulate their anti-inflammatory, immunomodulatory and anti-infective benefits, suggesting a bidirectional interaction (Pagnini *et al.,* 2021; Bishop *et al.,* 2020).

While models describing the microbiome (Magnúsdóttir & Thiele, 2018; Kumar *et al.,* 2019, Shashkova *et al.*, 2016; Adrian, 2020), vitamin D metabolism (Chun *et al.,* 2012, Beentjes *et al.,* 2019), the immune system in response to pathogens (Stübler *et al.,* 2023) and coupled microbe-immune system interaction (Hara & Iwasa, 2019) are available in the literature, the aim of this paper is to develop a novel mathematical model to describe for the first time the complex interactions between the microbiota, the intestinal barrier, vitamin D and the immune response in order to understand better the effects of

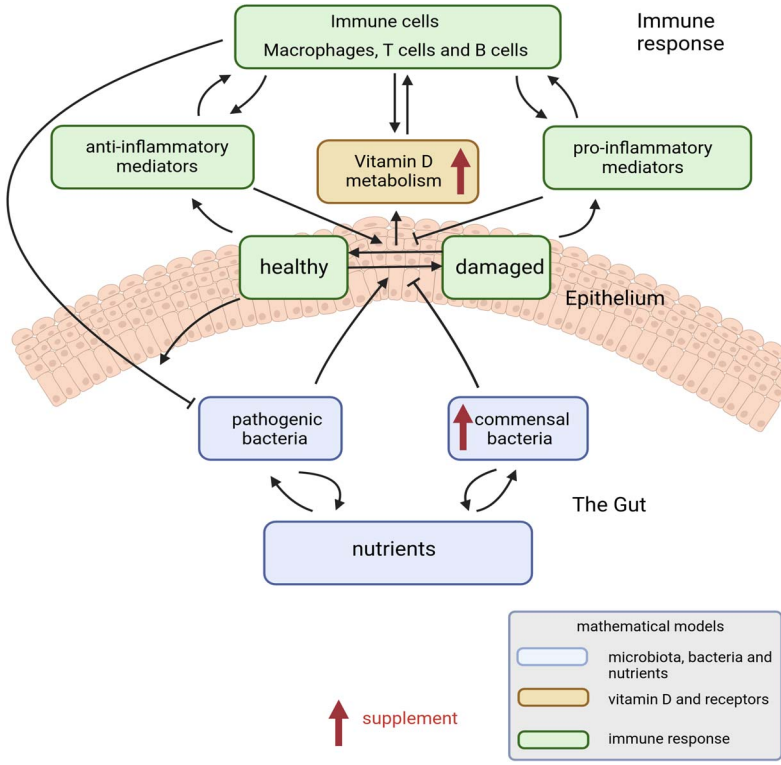

FIG. 1. The interactions between the microbiota, vitamin D and the immune response captured in the mathematical models presented in Sections 2.1, 2.2 and 2.3, respectively.

individual and co-supplementation of vitamin D and probiotics. The model seeks to be at a level of complexity appropriate to the nature of the biological components and available data.

The complete model is split into three sub-models. These are described, along with their parameter values for the intestinal nutrients and bacteria (Subsection 2.1), vitamin D and its metabolites (Subsection 2.2) and the epithelial barrier and immune response (Subsection 2.3), along with simulations with and without inflammation. We believe these individual models to be of interest in their own right and are combined in Section 3 and solved numerically to assess the impact of vitamin D supplements only (Subsection 3.2), probiotics only (Subsection 3.3) and co-supplementation (Subsection 3.4).

The full model will enable investigation into the proposed beneficial effects observed experimentally of combined supplementation, with the goal of determining whether they might improve human health.

2. Model formulation

The schematic shown in Fig. 1 summarizes the complex interactions between the three submodels i.e. the intestinal microbiota, vitamin D and the immune response captured by the model.

We begin by providing a detailed derivation and explanation of the mathematical equations for each of these processes individually. Baseline parameters and the sensitivity of the model to these are discussed

TABLE 1 *Description and units of the dependent variables in the full model.*

Variable	Description	Units	Variable	Description	Units
N_{ma}	Concentration of macronutrients	ng/ml	N_{mi}	Concentration of micronutrients	ng/ml
N_{mb}	Concentration of metabolites	ng/ml	N_a	Concentration of alternate nutrients	ng/ml
F	Population of commensal bacteria	CFU	P	Population of pathogenic bacteria	CFU
D	Extracellular concentration of 25(OH)D	ng/ml	D_a	Extracellular concentration of $1,25(OH)_2D$	ng/ml
D_i	Intracellular concentration of 25(OH)D	ng/ml	D_{a_i}	Intracellular concentration of $1,25(OH)_2D$	ng/ml
V_{D_a}	Concentration of VDR:$1,25(OH)_2D$ complex	ng/ml	E	Volume fraction of healthy epithelial cells	no units
E_d	Volume fraction of damaged epithelial cells	no units	M	Density of macrophages	cells/ml
			R	Density of regulatory cells	cells/ml
T_h	Density of T-helper cells	cells/ml	B	Density of plasma B cells	cells/ml
G	Concentration of anti-inflammatory cytokines	ng/ml	C	Concentration of pro-inflammatory cytokines	ng/ml
t	Time	days			

for each sub-model and simulations presented to verify behaviour. We then consider the full model, combining the three model components, to predict the effect of vitamin D and probiotic interventions on the system. The code, in the form of a R notebook, for these latter simulations is provided in the supplementary material. ODEs were solved using the ode solver in R with the default integrator lsoda.

A summary of each dependent variable in the model, along with its units, is given in Table 1.

2.1 *The microbiota*

The microbiota consists of several groups of microorganisms, including bacteria, archaea, yeast and viruses. In our model we simplify to include two populations of bacteria, namely commensals F (of which over 90% are represented by the two phyla Firmicutes and Bacteroidetes) and pathogenic bacteria P (such as *Salmonella* and invasive *E. coli*).

Interactions between bacteria, nutrients and epithelial cells are described in Fan & Pedersen (2021), Pickard *et al.* (2017) and Zhou *et al.* (2022) and summarized as follows: macronutrients N_{ma} (e.g. carbohydrates, protein, fat, fibre) and micronutrients N_{mi} (e.g. vitamins and minerals) are consumed from the diet at rates N^0_{ma} and N^0_{mi}, respectively, with intestinal microbes and epithelial cells competing for the latter at rates η_3 (commensals), η_4 (pathogens) and η_5 (epithelial cells). Commensal bacteria principally convert macronutrients by fermentation into metabolites N_{mb} (e.g. SCFAs) at rate η_1, most of these metabolites being absorbed by the intestinal mucosa, both providing important fuel for the proliferation of intestinal epithelial cells (rate η_6) and having beneficial effects on immune cells through induction of intracellular or extracellular processes. Metabolites support epithelial barrier integrity and function through induction of genes encoding tight junction components and exert anti-inflammatory effects in the intestinal mucosa by inducing anti-inflammatory cytokines. Gases (e.g. hydrogen and methane) are also produced during fermentation, which can be utilized by some commensal microbes at rate η_7 while

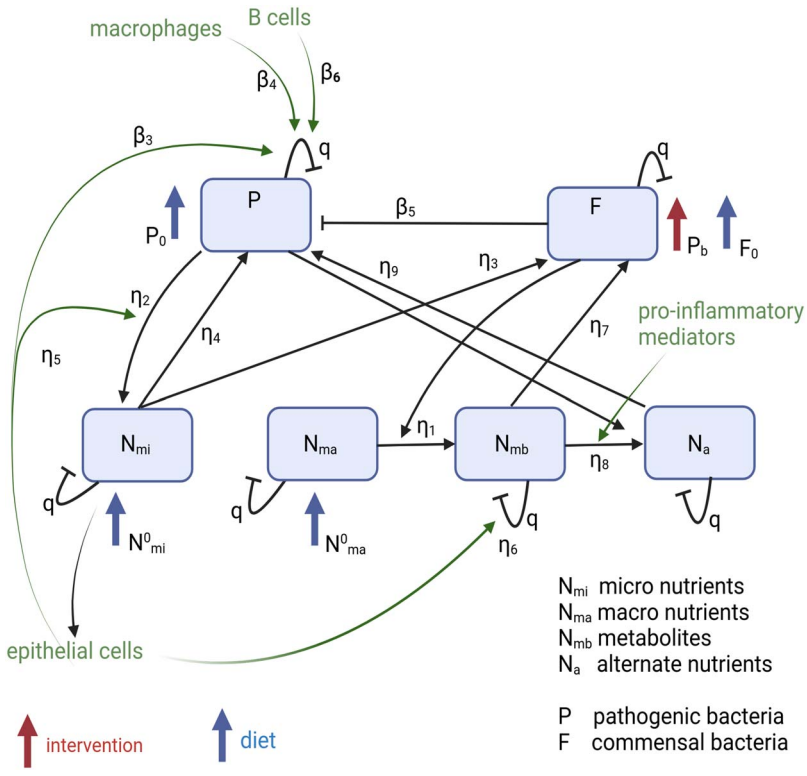

FIG. 2. **The microbiota and nutrient network.** The model derived in equations (2.1)–(2.6) captures the reactions between commensal and pathogenic bacteria, macronutrients, micronutrients, metabolites and alternate nutrients. The rates are defined in Table 2.

other gases need to be expelled (e.g. hydrogen sulphide). Pathogens induce intestinal inflammation and use virulence factors or toxins to enable conversion of metabolic byproducts generated by commensal bacteria into alternate nutrients N_a (e.g. carbohydrates, ethanolamine) at rate η_8. Some toxins (e.g. Shiga toxin) can also directly rupture the epithelial barrier, but we do not consider this mechanism here. The alternate nutrients are utilized as an energy source by pathogenic bacteria at rate η_9, giving them an advantage over commensals as they lack this ability. If pathogenic bacteria bypass or avoid microbiota-based defences to reach host cells, they can be taken up by the cells via endocytic pathways and degraded by phagolysosomes, releasing micronutrients from the breakdown of the cell components at rate η_2. Autophagy plays a role in this mechanism and is regulated by the gene ATG16L1 and can be induced by SCFAs (Bakke *et al.*, 2018). We assume that excess macronutrients, micronutrients, metabolites and alternate nutrients are removed from the gastrointestinal tract in the faeces or flatulence at the same rate q. A summary of these interactions is shown in Fig. 2.

The equations governing the concentrations of the different nutrient types are then

$$\frac{dN_{ma}}{dt} = N^0_{ma} - \eta_1 F N_{ma} - q N_{ma}, \tag{2.1}$$

$$\frac{dN_{mi}}{dt} = N^0_{mi} + \eta_2 N_{mb} E P - \eta_3 F N_{mi} - \eta_4 P N_{mi} - \eta_5 E N_{mi} - q N_{mi}, \tag{2.2}$$

$$\frac{dN_{mb}}{dt} = \eta_1 F N_{ma} - \eta_6 E N_{mb} - \eta_7 F N_{mb} - \eta_8 N_{mb} C P - q N_{mb}, \tag{2.3}$$

$$\frac{dN_a}{dt} = \eta_8 N_{mb} C P - \eta_9 N_a P - q N_a, \tag{2.4}$$

where E represents the volume fraction of epithelial cells that are healthy, with tight junctions between them (so that $E = 1 - E_d$ where E_d is the volume fraction of damaged epithelial cells) and C denotes the concentration of pro-inflammatory mediators, which we assume to be a measure of inflammation. We assume in this sub-model that they are both constant. Over 90% of SCFAs produced by the intestinal microbiota are absorbed by the mucosa to support the growth and proliferation of epithelial cells (Conlon & Bird, 2014) so we assume that $\eta_6 E \gg \eta_7 F$ and $\eta_8 CP$.

We assume that commensal and pathogenic bacteria acquired from diet and the environment enter the intestinal tract at rates F^0 and P^0, respectively. We include an additional input term for the commensal bacteria population to incorporate probiotic supplementation at rate P_b. Probiotics are identified by specific strains (e.g. *Lactobacillus*, *Bifidobacterium*) that influence the intestinal microbiota in different ways. Here we assume that they increase the number of commensals, which will enhance the production of beneficial bioactive metabolites. We assume that commensal bacteria proliferation depends upon availability of micronutrients and metabolites (converted from macronutrients) and the rates of proliferation are proportional to the consumption rates η_3 and η_7, respectively, with proportionality constant β_1. The pathogenic bacteria also compete for the micronutrients and utilize these and the alternate nutrients (converted from metabolites) for proliferation at rates proportional to their rates of consumption η_4 and η_9, respectively, with proportionality constant β_2.

In addition, commensal microbes mediate pathogen colonization resistance by producing toxic/ antimicrobial substances e.g. bacteriocins, secondary bile acids and fermentation products such as SCFAs and AMPs that directly inhibit the growth of pathogens at rate β_5. Commensals also enhance intestinal barrier function via their impact on tight junction proteins and mucus production and induce AMP production by epithelial cells and autophagy to destroy pathogens at rate β_3. They also activate the immune response by stimulating innate phagocytic cells (e.g. macrophages) to produce AMPs and recruit other innate and adaptive immune cells to contain and eradicate pathogens at rate β_4. Activated mucosal plasma B cells produce antibodies, specifically immunoglobulin A (IgA), which is transported by intestinal epithelial cells into the mucus layer where it becomes secretory IgA (sIgA). sIgA coats pathogens, directly hindering their function and facilitates recognition and subsequent elimination of pathogens by innate immune cells at rate β_6. Note that we do not include adhesion or niche exclusion in our model. Commensal and pathogenic bacteria are removed from the system by degradation or flushed out in the faeces and we assume this happens at the same rate as the excess nutrient removal i.e. q.

The equations governing the number of bacteria in the two populations are then given by

$$\frac{dF}{dt} = F^0 + P_b + f(B_T)\beta_1(\eta_3 N_{mi} + \eta_7 N_{mb})F - qF, \tag{2.5}$$

$$\frac{dP}{dt} = P^0 + f(B_T)\beta_2(\eta_4 N_{mi} + \eta_9 N_a)P - \beta_3 EP - \beta_4 MP - \beta_5 FP - \beta_6 BP - qP, \tag{2.6}$$

where M denotes the density of macrophages, B the density of activated plasma B cells (both assumed constant in this sub-model) and the dimensionless growth function $f(B_T)$, defined by

$$f(B_T) = 1 - \frac{B_T}{K}$$

represents logistic growth with carrying capacity K so that the growth of the total population density of bacteria $B_T = F + P$ has a maximum size K, which can be sustained in the intestine given the resources available.

We assume the microbiota are in homeostasis and consist mainly of commensal bacteria at $t = 0$, i.e.

$$N_{ma_0} = N_{ma_{ss}}, \quad N_{mi_0} = N_{mi_{ss}}, \quad N_{mb_0} = N_{mb_{ss}}, \quad N_{a_0} = N_{a_{ss}}, \quad F_0 = 0.99 \times 10^{14}, \quad P_0 = 0.01 \times 10^{14}, \tag{2.7}$$

where subscript $_{ss}$ denotes the nutrient concentration at steady state.

2.1.1 *Parameter values and sensitivity analysis for microbiome model.* Parameter values are not readily available. However, we can make estimates for the consumption rate of macronutrients N^0_{ma}, micronutrients N^0_{mi}, commensal F^0 and pathogenic bacteria P^0, the rate of removal of these in the faeces q and also the carrying capacity K (see Table 2). Note that we do not take into account the gastrointestinal transit times. From clinical studies we also know approximate rates of intake of probiotics P_b. The number of microbes consumed in the diet is given in Lang *et al.* (2014) as 1.3×10^9 CFU/day and we assume that pathogenic bacteria make up approximately 5% of the total intake. We also assume that the daily intake of macronutrients and micronutrients, the rate of removal of nutrients and bacteria in the faeces and the daily intake of commensal and pathogenic bacteria are all proportional. These are summarized, along with estimates for the remaining parameters not available in the literature, in Table 2. These have been chosen to produce biologically realistic results.

Given the considerable uncertainty in the choice of parameter values, a standard local sensitivity analysis is performed to analyse the effects of changing the individual parameters on the nutrient concentrations and bacterial populations. The following method is also applied to the vitamin D and vitamin D receptor, epithelial barrier and immune response models described in Sections 2.2.1 and 2.3.1.

Method for sensitivity analysis. Using the baseline parameter values in Table 2, we solve our system of ODEs (2.1)–(2.6) to large time to determine the nutrient concentrations and bacterial populations at steady state. We then estimate the local effect of parameters on these steady states by increasing and decreasing each parameter individually by 10%, and again, solving to large time to determine the new steady state. The sensitivity is then calculated by the relative change in our output variable at steady state in relation to the relative change in the parameter i.e.

$$\text{Sensitivity} = \frac{\Delta \mathbf{y}/\mathbf{y}}{|\Delta\theta|/\theta}, \tag{2.8}$$

where $\mathbf{y}$ is the output variable, i.e. $N_{ma}, N_{mi}, N_{mb}, N_a, F$ and P, and θ is the parameter so that $\Delta\theta = 1.1\times\theta$ and $\Delta\theta = 0.9 \times \theta$. This provides a measure of how much the concentration of nutrients or number of bacteria increase or decrease in relation to an up- or down-regulation in the parameter value.

We assume that values for the volume fraction of healthy epithelial cells E, macrophage density M, pro-inflammatory cytokine concentration C and plasma B cell density B are constant i.e.

$$E = 0.9, \quad C = 0.45 \text{ pg/ml}, \quad M = 4.9 \times 10^5 \text{ cells/ml}, \quad B = 3.8 \times 10^3 \text{ cells/ml},$$

representing low levels of inflammation in which the epithelial barrier is compromised, increasing signalling of pro-inflammatory cytokines that activate macrophages and B cells. Concentrations and

TABLE 2 *Definition, value and units of the nutrient model parameters. In developed countries, adults consume on average approximately 400 g/day of macronutrients and 9 g/day of micronutrients (Salazar et al., 2019). They typically expel 128 g/day of faeces of which there are approximately 1×10^{11} bacteria/g of wet stool so that the total number of bacteria removed in the faeces is 1.28×10^{13} bacteria/day^{-1} (Sender et al., 2016). Expressing this in terms of the total number of bacteria in the intestine gives an approximate value of $q = 0.13$ day^{-1}. In a healthy diet we consume approximately 1.3×10^{9} CFU/day (Lang et al., 2014) and we assume 5% of these microbes are pathogenic. There are approximately 1×10^{14} CFU of bacteria in the intestinal tract so we assume that the carrying capacity K equals this value.*

Parameter	Description	Value	Units
N^0_{ma}	Rate of intake of macronutrients	400	g/day
N^0_{mi}	Rate of intake of micronutrients	9	g/day
q	Rate of faecal removal of excess nutrients and bacteria	0.13	day^{-1}
F^0	Rate of intake of commensal bacteria	1.24×10^{9}	CFU/day
P^0	Rate of intake of pathogenic bacteria	0.06×10^{9}	CFU/day
P_b	Rate of intake of probiotics	1×10^{9}-1×10^{11}	CFU/day
K	Carrying capacity	1×10^{14}	CFU
η_1	Rate of uptake of macronutrients by commensal bacteria	1×10^{-14}	(CFU.day)$^{-1}$
η_2	Rate of release of micronutrients from degradation of pathogenic bacteria	1×10^{-17}	(CFU.day)$^{-1}$
η_3	Rate of consumption of micronutrients by commensal bacteria	1×10^{-14}	(CFU.day)$^{-1}$
η_4	Rate of uptake of micronutrients by pathogenic bacteria	1×10^{-14}	(CFU.day)$^{-1}$
η_5	Rate of consumption of micronutrients by host epithelial cells	0.01	day^{-1}
η_6	Rate of utilization of metabolites by epithelial cells	0.1	day^{-1}
η_7	Rate of utilization of metabolites by commensal bacteria	1×10^{-17}	(CFU.day)$^{-1}$
η_8	Rate of production of alternate nutrients	1.3×10^{-9}	ml/(ng.CFU.day)
η_9	Rate of consumption of alternate nutrients by pathogens	1×10^{-14}	(CFU.day)$^{-1}$
β_1	Proportionality parameter	2.44×10^{5}	CFU/ng
β_2	Proportionality parameter	2.44×10^{4}	CFU/ng
β_3	Rate at which pathogenic bacteria are destroyed by autophagy and AMPs from epithelial cells	0.5	day^{-1}
β_4	Rate at which pathogens are destroyed by macrophages	9.17×10^{-9}	ml/day
β_5	Rate at which pathogens are destroyed by commensals	1×10^{-17}	(CFU.day)$^{-1}$
β_6	Rate at which pathogens are destroyed by sIgA	1.03×10^{-6}	ml/day

densities have been approximated to be half the measured values from in-house human data on the pro-inflammatory cytokine IFN-γ, plasma B cells and macrophages in blood in diseased individuals experiencing inflammation.

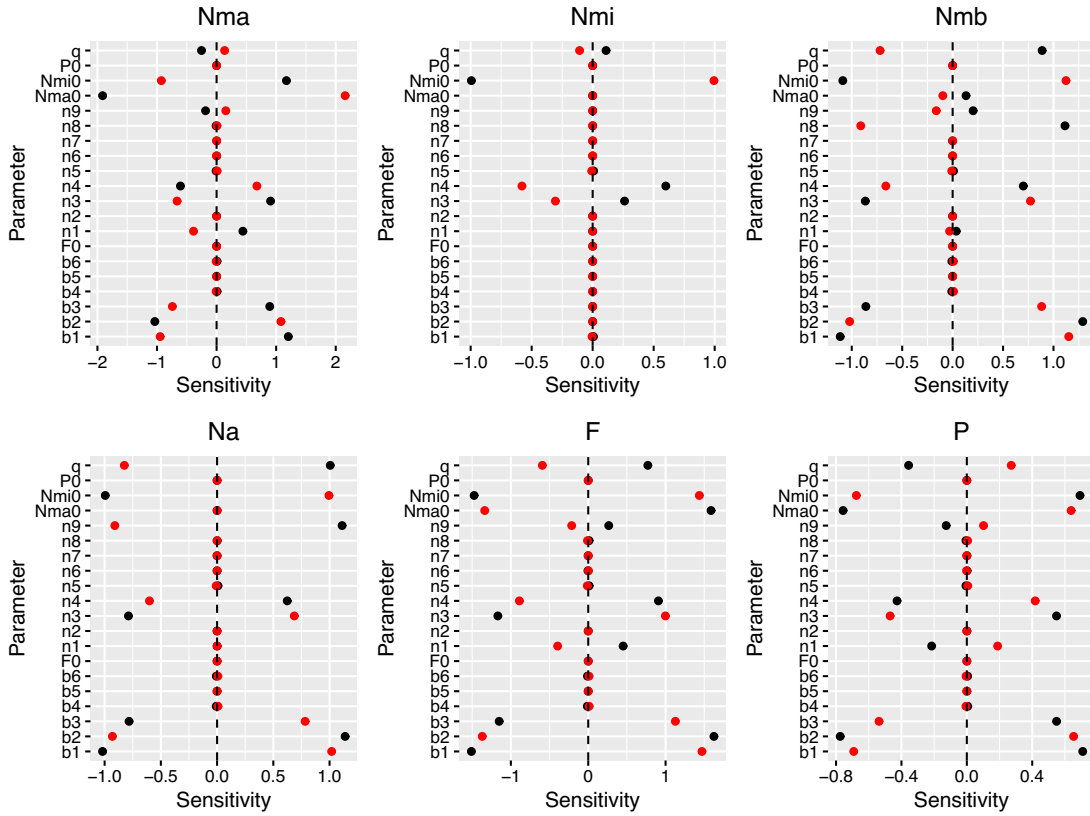

FIG. 3. The effect of varying parameter values on the steady state concentrations of macronutrients, micronutrients, metabolites and alternate nutrients and the number of commensal and pathogenic bacteria. Baseline parameter values are taken from Table 2 and each parameter is sequentially varied by a 10% decrease (black) and a 10% increase (red). Sensitivity is defined by equation (2.8). We assume low levels of inflammation so $E = 0.9$, $C = 0.45$ pg/ml, $M = 4.9 \times 10^5$ cells/ml, $B = 3.8 \times 10^3$ cells/ml. Note that n=η and b=β.

Figure 3 demonstrates that the parameters that are the most influential on the bacterial populations are the rates of intake of micronutrients N^0_{mi} and macronutrients N^0_{ma}, proportionality parameters β_1 and β_2, the rate at which pathogenic bacteria are destroyed by autophagy and AMPs from epithelial cells β_3, the consumption of micronutrients by commensals η_3 and the rate of uptake of micronutrients by pathogenic bacteria η_4 and the rate of faecal removal q. A decrease in q, the rate of production of alternate nutrients η_8, η_4 and β_2 and an increase in N^0_{mi}, η_3, β_3 and β_1 results in an increase in metabolites, which are utilized by the commensal bacteria resulting in growth of the commensal population and a decline in pathogens. A decrease in N^0_{mi}, η_3, β_1, β_3, the rate of consumption of macronutrients by commensals η_1 and an increase in N^0_{ma}, β_2 and η_4 increases the concentration of macronutrients, which decreases the concentration of metabolites, inhibiting the commensal population. Similarly, a decrease in η_3 and η_4 and an increase in N^0_{mi} increases the concentration of micronutrients that are consumed by the pathogens, also inhibiting the commensal population.

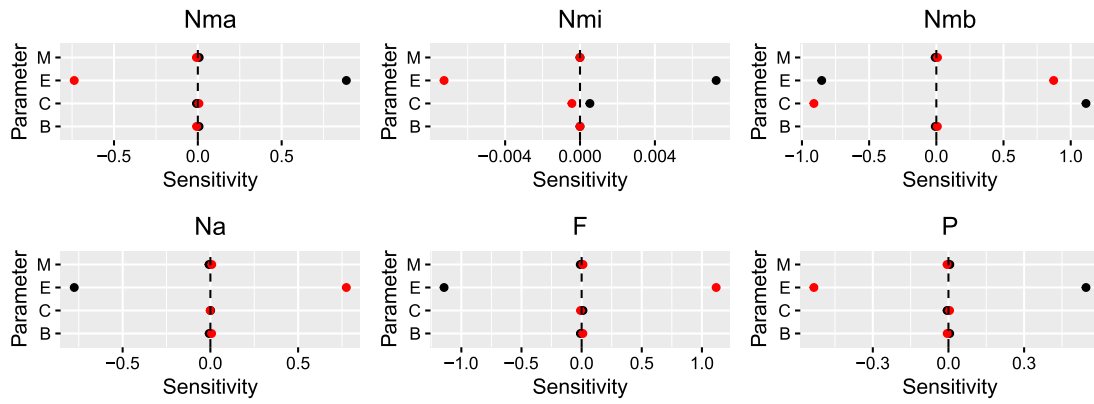

FIG. 4. The effect of varying parameter values on the steady state concentrations of macronutrients, micronutrients, metabolites and alternate nutrients and the number of commensal and pathogenic bacteria. Baseline parameter values are taken from Table 2 with E, B, C and M sequentially varied by a 10% decrease (black) and a 10% increase (red). Sensitivity is defined by equation (2.8).

The sensitivity of the model to the immune/inflammatory variables, i.e. E, C, M, B, is shown in Fig. 4 keeping the baseline parameters in Table 2 constant and increasing and decreasing the values for E, C, M and B above by 10%. All of the variables are sensitive to changes in the volume fraction of healthy epithelial cells, in particular, macronutrients, micronutrients and pathogens decline with an increase in E while metabolites, alternate nutrients and commensals increase. The concentration of metabolites is also influenced by the concentration of pro-inflammatory cytokines. The densities of macrophages and plasma B cells are not influential on the bacterial populations or nutrient concentrations for the specified changes of magnitude.

As the system of equations is too complicated to solve analytically for the steady state solutions, we also consider sensitivity of the model to a wide range of initial data to large time and Fig. 5 illustrates how the steady state values of the model variables change with an increasing initial pathogen population P_0 with the initial concentrations of nutrients and population of commensal bacteria remaining constant.

When the initial pathogen population exceeds a certain threshold (approximately $>1\times10^{12}$ CFU), the pathogenic bacteria dominate, utilizing the alternate nutrients to proliferate faster than the rate they are being destroyed by AMPs and the inflammatory response. This indicates that the system is bistable, suggesting that when the microbiome is in sufficient dysbiosis, it triggers the transition from a non-inflammatory to an inflammatory steady state.

Changes in initial nutrient concentrations and the population of commensals (not shown) do not influence the steady state values of N_{ma}, N_{mi}, N_{mb}, N_a, F and P.

2.1.2 *Model results for microbiota.* Using the parameter values in Table 2 and solving equations (2.1)–(2.6), Fig. 6 shows the predicted behaviour of the nutrient concentrations and bacteria populations over time with no probiotic supplementation and with and without inflammation. For simulations of a healthy state with no inflammation present, we assume that the concentration of pro-inflammatory cytokines $C = 0.27$ pg/ml, densities of macrophages and plasma B cells are $M = 3.4 \times 10^5$ cells/ml and $B = 2.6 \times 10^3$ cells/ml, respectively, with no damaged epithelial cells, i.e. $E = 1$. Under inflammatory conditions, C, M and B are upregulated and E is downregulated as the epithelial cells experience damage.

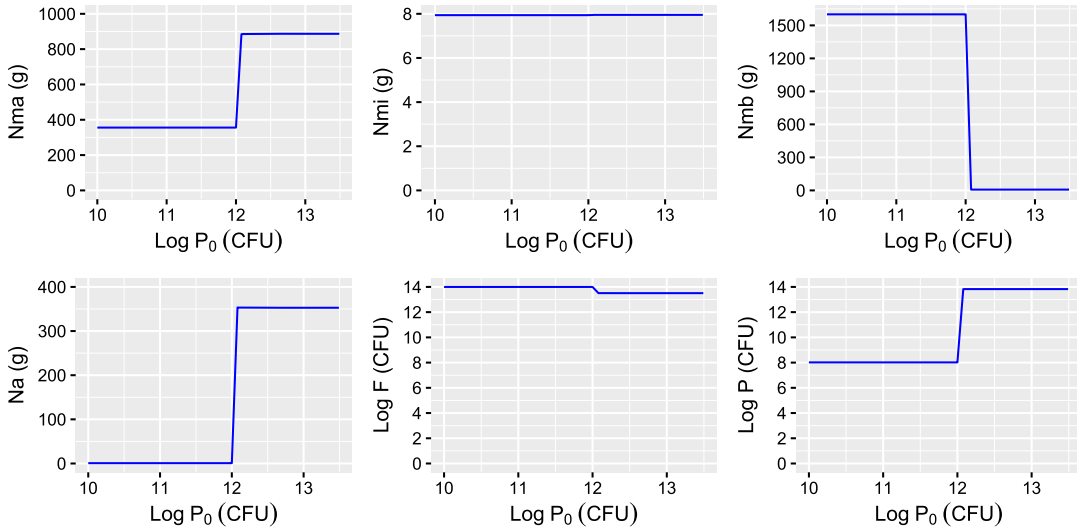

FIG. 5. The predicted steady state concentrations of nutrient and bacterial populations from solving equations (2.1)–(2.6) with baseline parameters given in Table 2 with increasing initial pathogen population P_0. As before, $E = 0.9$, $C = 0.45$ pg/ml, $M = 4.9 \times 10^5$ cells/ml, $B = 3.8 \times 10^3$ cells/ml. Initial conditions for N_{ma}, N_{mi}, N_{mb}, N_a and F are constant.

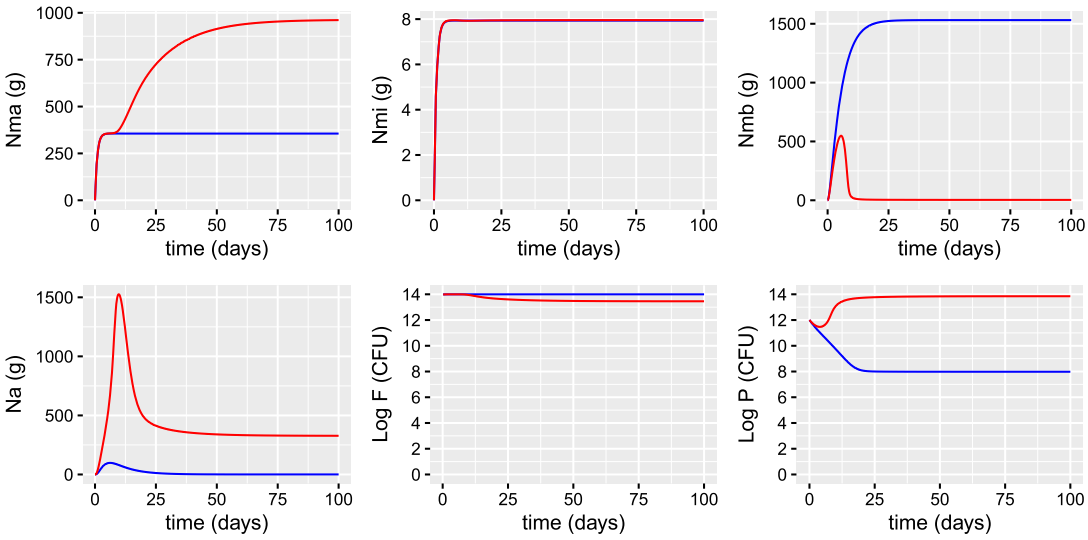

FIG. 6. Simulations predicting the concentrations of macronutrients N_{ma}, micronutrients N_{mi}, metabolites N_{mb}, alternate nutrients N_a and populations of commensals F and pathogens P from solving equations (2.1)–(2.6) with baseline parameter values given in Table 2 with (red line) and without (blue line) inflammation. $C = 0.27$ pg/ml, $M = 3.4 \times 10^5$ cells/ml, $B = 2.6 \times 10^3$ cells/ml and $E = 1$ for the non-inflammatory case and $C = 0.91$ pg/ml, $M = 9.8 \times 10^5$ cells/ml, $B = 7.6 \times 10^3$ cells/ml and $E = 0.8$ for the inflammatory case. Note that probiotic supplementation is not considered here, so $P_b = 0$.

In a healthy individual with no inflammation, the concentration of nutrients and bacterial populations attain a steady state. The concentration of alternate nutrients N_a is small, so that the commensal

bacteria dominate, utilizing the metabolites and micronutrients to proliferate and inhibiting the growth of pathogenic bacteria. Under inflammatory conditions, the population of pathogenic bacteria grows, resulting in fewer commensals to consume the macronutrients (hence the concentration of N_{ma} increases) and convert them into metabolites. The concentration of metabolites therefore decreases, providing less fuel for the intestinal epithelial cells, instead favouring conversion to alternate nutrients by the pathogenic bacteria. Pathogenic bacteria then utilize these alternate nutrients to proliferate at a rate greater than the rate at which they are eliminated by AMPs and the inflammatory response. The concentration of micronutrients remains almost unchanged.

2.2 *Vitamin D and the vitamin D receptor*

We assume that vitamin D (25(OH)D), denoted by D, is converted in the kidney by 1-α-hydroxylase (CYP27B1) into its active form 1,25-dihydroxyvitamin D ($1,25(OH)_2D$), represented by D_a. However, $1,25(OH)_2D$ can directly inhibit expression of CYP27B1 as a safeguard mechanism against hypercalcaemia (Tang *et al.,* 2019). Availability of 25(OH)D from the diet, supplements and sunlight is denoted by D^0. In Jones *et al.* (2013), it was shown that probiotic supplements increase serum concentrations of 25(OH)D in humans and can increase intestinal vitamin D absorption (Abboud *et al.,* 2020). We therefore include a saturating term involving the probiotics with maximum production rate δ_1. The equations governing the serum concentrations are

$$\frac{dD}{dt} = D^0\left(1 + \frac{\delta_1 P_b}{K_\delta + P_b}\right) - \frac{k_d D}{\delta(1 + D_a)(K_D + D)} - \delta_2 D, \tag{2.9}$$

$$\frac{dD_a}{dt} = \frac{k_d D}{\delta(1 + D_a)(K_D + D)} - \delta_3 D_a, \tag{2.10}$$

where $k_d/\delta(1+D_a)$ is the maximal rate of conversion of 25(OH)D to $1,25(OH)_2D$, K_D is the Michaelis–Menten constant, δ_2 is the rate of degradation and conversion to other metabolites of 25(OH)D and δ_3 is the degradation rate of $1,25(OH)_2D$.

As discussed in Chun *et al.* (2012), the serum vitamin D binding protein (DBP—this is the main serum carrier of vitamin D metabolites) and to a lesser extent, albumin, play a key role in the bioavailability of 25(OH)D and $1,25(OH)_2D$. Some functions of vitamin D are more closely correlated with levels of free 25(OH)D, rather than the total serum concentration. We therefore assume that the concentrations of free 25(OH)D and $1,25(OH)_2D$, denoted by D_f and D_{a_f}, respectively, are given by

$$D_f = \mu_f D, \qquad D_{a_f} = \mu_{a_f} D_a, \tag{2.11}$$

where μ_f and μ_{a_f} denote the proportions of total 25(OH)D and $1,25(OH)_2D$ that are free. Data presented in Chun *et al.* (2012) showed that for a physiological concentration of serum 25(OH)D (50 nM) and $1,25(OH)_2D$ (100 pM), the percentage of free 25(OH)D and $1,25(OH)_2D$ *in vivo* ranged from 0.026–0.074% and 0.4–1.3%, respectively.

We assume that free vitamin D and its metabolites can diffuse across the membrane from the extracellular space into the intracellular fluid of macrophages and vice versa, and likewise for epithelial cells lining the intestinal wall. The extracellular concentrations of 25(OH)D and $1,25(OH)_2D$ act as a source for intracellular levels of vitamin D metabolites but as the blood volume is much larger than the intracellular volume we assume (as in Chun *et al.,* 2012) that the extracellular levels are little

affected by intracellular dynamics. Intracellular 25(OH)D is converted into $1,25(OH)_2D$ via the enzyme CYP27B1 and both 25(OH)D and $1,25(OH)_2D$ bind to the vitamin D receptor (VDR), which functions as a transcription factor regulating gene expression. The magnitude of this response depends upon the concentration of ligand and receptor present. This is a key mechanism underpinning the innate antibacterial responses. However, 25(OH)D has a 500-fold lower affinity for VDR than $1,25(OH)_2D$, so we only consider the binding of $1,25(OH)_2D$ to the VDR. The intracellular concentrations of 25(OH)D, denoted by D_i and $1,25(OH)_2D$, denoted by D_{a_i} is governed by

$$\frac{dD_i}{dt} = (\mu_f D - D_i)(\sigma_1 M + \sigma_2 E) - \frac{k_{d_i} D_i}{\delta_i (1 + D_{a_i})(K_{D_i} + D_i)} - \delta_4 D_i, \tag{2.12}$$

$$\frac{dD_{a_i}}{dt} = (\mu_{f_a} D_a - D_{a_i})(\sigma_1 M + \sigma_2 E) + \frac{k_{d_i} D_i}{\delta_i (1 + D_{a_i})(K_{D_i} + D_i)} - \delta_5 D_{a_i}, \tag{2.13}$$

where $k_{d_i}/\delta_i(1 + D_{a_i})$ is the maximal rate of conversion of intracellular 25(OH)D to $1,25(OH)_2D$, K_{D_i} is the Michaelis–Menten constant, σ_1 and σ_2 are the permeabilities of macrophages and epithelial cells, respectively, to the vitamin D metabolites, δ_4 is the rate of degradation and conversion to other metabolites of intracellular 25(OH)D and δ_5 is the degradation rate of intracellular $1,25(OH)_2D$. M and E represent the density of macrophages and volume fraction of epithelial cells present. It should be noted that T cells and B cells do not express VDR until they are stimulated with a mitogen or antigen (pathogenic or commensal) and, therefore, there appears to be a threshold for activation of intracellular $1,25(OH)_2D$ (Karmali *et al.,* 1991). However, we do not include this complexity.

We assume that V_{D_a} represents the complex VDR:$1,25(OH)_2D$ that is responsible for inducing the cellular response. The most sensitively regulated gene for $1,25(OH)_2D$-VDR is CYP24A1, which encodes the enzyme 24-hydroxylase. This acts as a feedback mechanism to convert $1,25(OH)_2D$ to $1,24,25(OH)_3D$, which is a much less active vitamin D metabolite and binds to VDR with lower affinity (Chun *et al.,* 2012). $1,25(OH)_2D$ therefore actively promotes its own inactivation and we encompass this into the last term in the equation

$$\frac{dV_{D_a}}{dt} = \delta_6 D_{a_i} V - \delta_7 V_{D_a}. \tag{2.14}$$

Here δ_6 is the rate at which $1,25(OH)_2D$ binds to the VDR, V is the concentration of VDR and δ_7 is the rate of conversion or degradation.

Probiotics increase VDR protein expression and transcriptional activity, which regulates host response to invasive pathogens (i.e. upregulates function of intestinal epithelial barrier, production of AMPs from epithelial cells and immune cells and autophagy and downregulates pro-inflammatory cytokines) and commensal bacteria in innate and adaptive immunity (Vos *et al.,* 2017, Mujagic *et al.,* 2017, Stojanov *et al.,* 2020). In Lu *et al.* (2020) a single dose of probiotic resulted in an increase in VDR and autophagy signalling and inhibited inflammation. In our model, the concentration of VDR, V, is therefore assumed to depend upon the intake of probiotics P_b so that it takes the saturating form

$$V = \frac{\delta_8 (a + P_b)}{P_b + K_V}, \tag{2.15}$$

where $V = \delta_8 a/K_V$ when $P_b = 0$. A summary of these interactions is shown in Fig. 7.

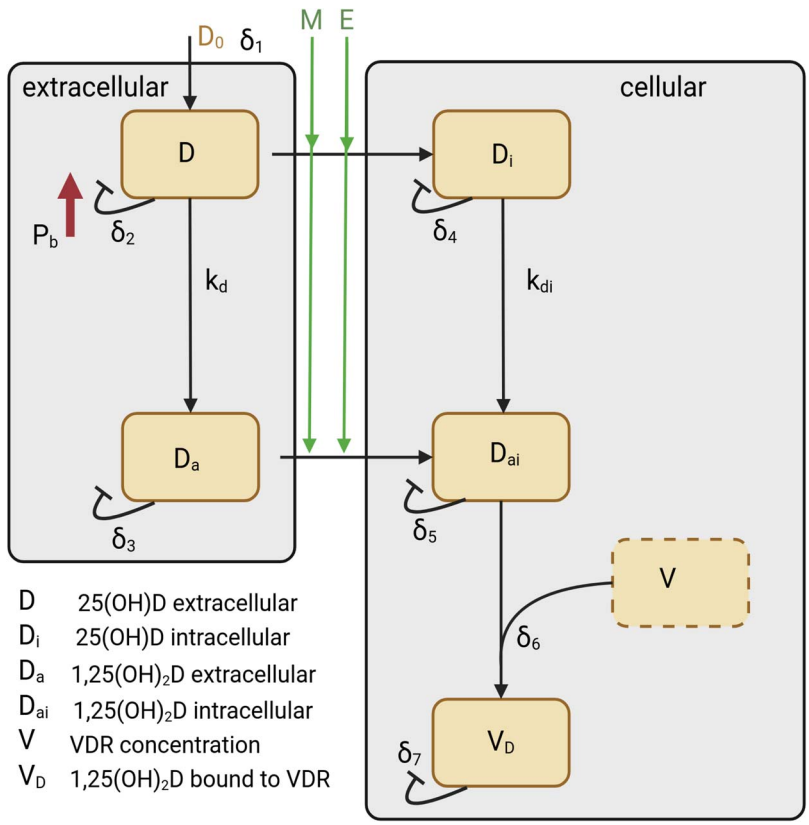

FIG. 7. **The vitamin D network.** The model derived in equations (2.9)–(2.14) describes the conversion of 25(OH)D into its active form $1,25(OH)_2D$, the diffusion of the free forms of these across the epithelial and macrophage cell membranes and the binding with the vitamin D receptor. The rates are defined in Table 3.

We assume that at time $t = 0$ the concentration of serum 25(OH)D is constant and the concentrations of its metabolites are at steady state, i.e.

$$D_0 = D_{ss}, \quad D_{a_0} = D_{a_{ss}}, \quad D_{i_0} = D_{i_{ss}}, \quad D_{a_{i_0}} = D_{a_{i_{ss}}}, \quad V_{D_{a_0}} = V_{D_{a_{ss}}}. \tag{2.16}$$

2.2.1 *Parameter values and sensitivity analysis for vitamin D model.* Most parameter values are available from Chun *et al.* (2012) and Beentjes *et al.* (2019). The remainder were estimated to obtain results similar to measurements from experimental studies in the literature. A summary of values with units and references is given in Table 3.

Employing a similar method to that described in Subsection 2.1.1, using constant values for the volume fraction of healthy epithelial cells E and macrophage density M, indicates that the concentration of vitamin D and its metabolites is dependent upon several different parameters (see Fig. 8). All of the variables are sensitive to the rate of intake of 25(OH)D by diet and sunlight D^0, the maximum production rate of vitamin D dependent upon probiotics δ_1, the degradation of 25(OH)D δ_2, the

TABLE 3 *Definition, value and units of the vitamin D model parameters. Note that 1 nM of 25(OH)D = 2.5 ng/ml.*

Parameter	Description	Value & Units	Reference
D^0	Production of 25(OH)D from diet and sunlight	variable nM/day	
k_d/δ	Maximal rate of conversion of extracellular 25(OH)D to $1,25(OH)_2D$	24 nM/day	Chun *et al.* (2012)
K_D	Michaelis–Menten constant for extracellular 25(OH)D binding to CYP27B1	1000 nM	Chun *et al.* (2012)
δ_1	$D^0\delta_1$ is the maximum production rate of vitamin D dependent upon probiotics	0.3	
δ_2	Degradation of extracellular 25(OH)D	$0.048\ \text{day}^{-1}$	Beentjes *et al.* (2019)
δ_3	Degradation of extracellular $1,25(OH)_2D$	$14.4\ \text{day}^{-1}$	Beentjes *et al.* (2019)
μ_f	Proportion of total extracellular 25(OH)D that is free	0.05 %	Chun *et al.* (2012)
μ_{a_f}	Proportion of total extracellular $1,25(OH)_2D$ that is free	0.85 %	Chun *et al.* (2012)
σ_1	Permeability of macrophages to free 25(OH)D or $1,25(OH)_2D$	$144\ \text{day}^{-1}$	Chun *et al.* (2012)
σ_2	Permeability of epithelial cells to free 25(OH)D or $1,25(OH)_2D$	$144\ \text{day}^{-1}$	
k_{d_i}/δ	Maximal rate of conversion of intracellular 25(OH)D to $1,25(OH)_2D$	24 nM/day	Chun *et al.* (2012)
K_{D_i}	Michaelis–Menten constant for intracellular 25(OH)D binding to CYP27B1	1000 nM	Chun *et al.* (2012)
δ_4	Degradation of intracellular 25(OH)D	$0.048\ \text{day}^{-1}$	Beentjes *et al.* (2019)
δ_5	Degradation of intracellular $1,25(OH)_2D$	$14.4\ \text{day}^{-1}$	Beentjes *et al.* (2019)
δ_6	Rate at which $1,25(OH)_2D$ binds to VDR	24×10^{-7} $\text{nM}^{-1}\text{day}^{-1}$	Chun *et al.* (2012)
δ_7	Rate of degradation of VDR:$1,25(OH)_2D$	$0.024\ \text{day}^{-1}$	
$\delta_8 a/K_V$	Concentration of VDR	1.2 nM	Chun *et al.* (2012)
K_V	Saturation constant	1 CFU/day	
K_δ	Saturation constant	5×10^8 CFU/day	

Michaelis–Menten constant for extracellular 25(OH)D binding to CYP27B1 K_D and the maximal rate of conversion of extracellular 25(OH)D to $1,25(OH)_2D$ k_d. The intracellular and extracellular concentrations of $1,25(OH)_2D$ and VDR:$1,25(OH)_2D$ complex are also dependent upon the degradation rate of $1,25(OH)_2D$ δ_3. The intracellular metabolites D_i and D_{a_i} are influenced by the proportion of their extracellular versions that are free i.e. μ_f and μ_{a_f}, respectively. The concentration of the VDR:$1,25(OH)_2D$ complex is also sensitive to the latter, in addition to the rate at which $1,25(OH)_2D$ binds to VDR δ_6, the rate of degradation of VDR:$1,25(OH)_2D$ δ_7 and the concentration of VDR δ_8. None of the variables depend upon $s = \sigma_1 = \sigma_2$, which could be interpreted as the change in the term $M + E$, and the model is insensitive to changes in initial conditions.

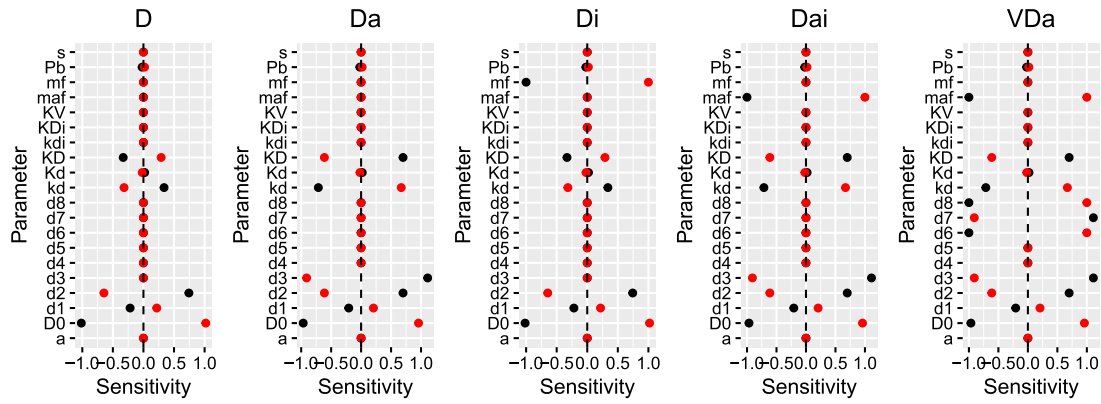

FIG. 8. The effect on varying parameter values on the steady state concentrations of extra- and intra-cellular 25(OH)D, 1,25$(OH)_2$D and the complex VDR:1,25$(OH)_2$D. Baseline parameter values are taken from Table 3 and each parameter is sequentially varied by a 10% decrease (black) and a 10% increase (red). Sensitivity is defined by equation (2.8) and s represents the permeability of macrophages and epithelial cells to 25(OH)D and 1,25$(OH)_2$D i.e. s=σ_1=σ_2. The volume fraction of epithelial cells $E = 0.9$ and density of macrophages $M = 4.9 \times 10^5$ cells/ml. Note that m=μ and d=δ.

2.2.2 *Model results for vitamin D/VDR pathway.* We solve equations (2.9)–(2.14) using the parameter values given in Table 3 for vitamin D and its metabolites. Vitamin D intake D^0 is chosen to represent production of 25(OH)D from diet and sunlight only (no supplements) and $P_b = 0$, representing no daily supplement of probiotics. Figure 9 shows the predicted concentrations over time with and without inflammation.

Under non-inflammatory conditions (i.e. when the density of macrophages $M = 3.4 \times 10^5$ cells/ml and the volume fraction of healthy epithelial cells $E = 1$), the concentrations of serum and intracellular 25(OH)D and 1,25$(OH)_2$D and VDR:1,25$(OH)_2$D complex remain constant. As reported in Tang *et al.* (2019) and Souberbielle *et al.* (2016), there is an approximate 1000-fold difference between the serum concentrations of 25(OH)D and its metabolite, which is also predicted by our model. Under inflammatory conditions, the density of macrophages M increases and the volume fraction of healthy epithelial cells decreases so that $M > 3.4 \times 10^5$ and $E < 1$. This increases the magnitude of the term $(\sigma_1 M + \sigma_2 E)$ as there are overall more cells that 25(OH)D and 1,25$(OH)_2$D can enter and bind to the vitamin D receptor. The local sensitivity analysis presented in Section 2.2.1 suggests that an increase in this term has a negligible effect on the levels of 25(OH)D and its metabolites. This is also demonstrated in Fig. 9.

2.3 *The intestinal epithelial barrier and the immune response*

We recall that epithelial cells are either healthy or damaged, so that the sum of their volume fractions

$$E + E_d = 1. \tag{2.17}$$

SCFAs (metabolites) provide energy for the proliferation of epithelial cells at rate ϵ_1 and VDR expression (which is enhanced by probiotics) upregulates the epithelial barrier function at rate ϵ_2 through induction of genes encoding tight junction components. However, pro-inflammatory mediators and toxins from inflowing pathogenic bacteria damage the epithelial cells at rate ϵ_4 and ϵ_5, respectively,

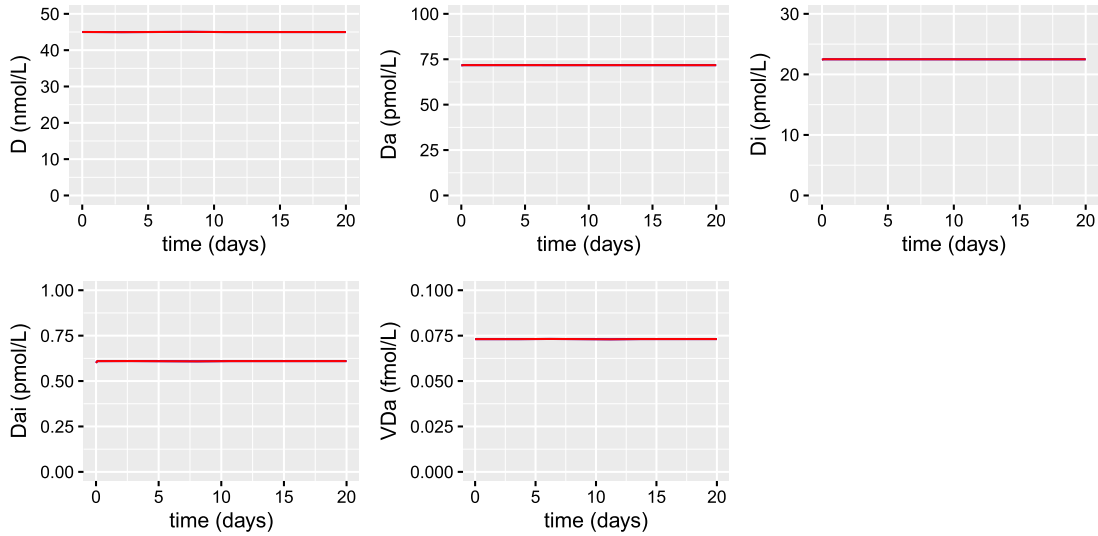

FIG. 9. Simulations predicting the effect of inflammation on the concentrations of extracellular and intracellular 25(OH)D and $1,25(OH)_2D$ and of the VDR:$1,25(OH)_2D$ complex from solving equations (2.9)–(2.14) with baseline parameter values given in Table 3. The density of macrophages increases from $M = 3.4 \times 10^5$ (blue) to $M = 9.8 \times 10^5$ cells/ml (red) and the volume fraction of healthy epithelial cells decreases from $E = 1$ (blue) to $E = 0.8$ (red). Supplementation is not considered here, so $P_b = 0$ and $D^0 = 3.2$ nM/day (8 ng/ml day^{-1}), which represents intake of vitamin D from diet and sunlight only.

with macrophages removing damaged cells at rate ϵ_3. We therefore have

$$\frac{dE}{dt} = \epsilon_1 N_{mb} E_d + (\epsilon_2 V_{D_a} + \epsilon_3 M) E_d - \epsilon_4 CE - \epsilon_5 PE, \tag{2.18}$$

$$\frac{dE_d}{dt} = \epsilon_4 CE + \epsilon_5 PE - (\epsilon_2 V_{D_a} + \epsilon_3 M) E_d - \epsilon_1 N_{mb} E_d. \tag{2.19}$$

The microbiota are involved in the training and development of major components of the host's innate and adaptive immune systems (Zheng *et al.,* 2020). A multitude of immune cells play a role in maintaining the integrity of the intestinal barrier and the model is restricted to include macrophages (density M), T-helper cells (density T_h), plasma B cells (density B) and a combined regulatory T and B cell density term R, which dampens down the immune response. It is important to include all these individual cell terms due to their specific functions in modifying, via the vitamin D receptor, the immune response. For example (as detailed in Subsection 2.2 and the model formulation below), antigen-presenting cells such as macrophages intracellularly convert 25(OH)D to active $1,25(OH)_2D$. This may then act locally (intracrine) to modify macrophage function via the vitamin D receptors expressed by the same cells. The VDR:$1,25(OH)_2D$ complex released by macrophages may also affect adjacent T and B cells by promoting regulatory cell function and inhibiting T-helper and plasma B cell proliferation (Lopez *et al.,* 2021). The model has been established to incorporate these cell-specific differences.

Epithelial and immune cells release a variety of chemokines and cytokines that have a range of functions. We consider here generic pro-inflammatory-type and anti-inflammatory-type cytokines

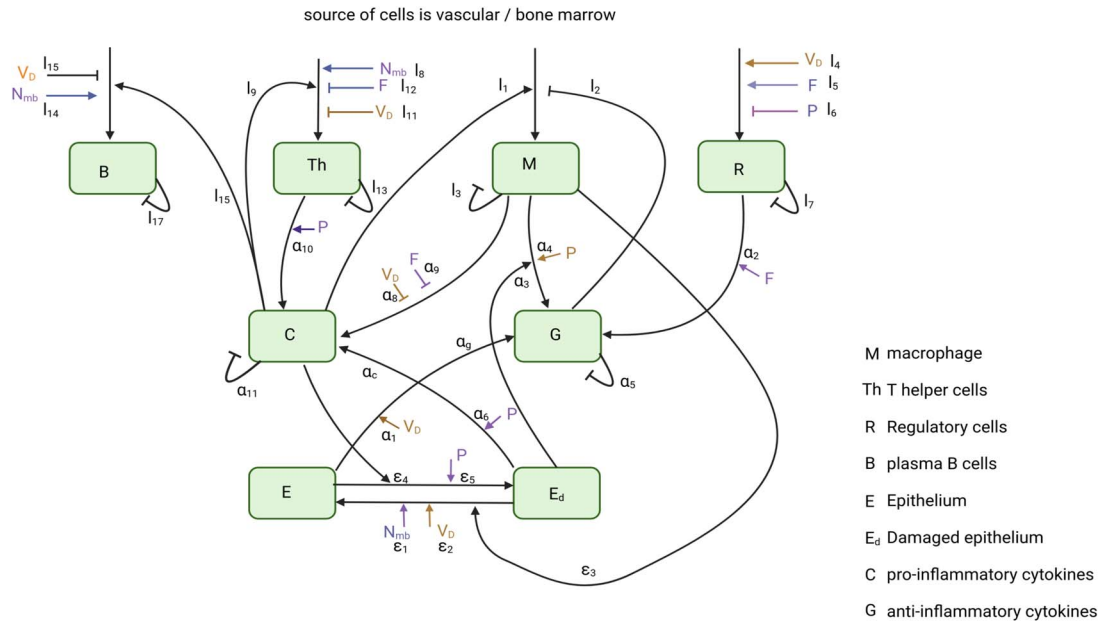

FIG. 10. **The immune response network.** The model derived in equations (2.18)–(2.25) details the interactions between the intestinal epithelial barrier and the innate and adaptive immune responses. The parameters are defined in Tables 4 and 5.

denoted by C and G, respectively. A summary of the interactions between these components is shown in Fig. 10.

Innate immune response. Intestinal mucosal macrophages are positioned in the subepithelial lamina propria where they can regulate inflammatory responses to bacteria that breach the epithelium, protect the mucosa against harmful pathogens and scavenge dead cells and foreign debris (Smith *et al.,* 2011). These macrophages exhibit greater phagocytic ability than other macrophages and under healthy conditions lack the normal pro-inflammatory cytokine release that can be switched in disease (Smith *et al.,* 2011). Pathogenic bacteria stimulate priming of intestinal macrophages through pro-inflammatory cytokines (rate ι_1) that promote recruitment of neutrophils to the site of infection, which eradicate the pathogens. Macrophages are long lived, dying (or migrating) after weeks or months (rate ι_3), this rate increasing under inflammatory conditions (De Maeyer *et al.,* 2021). Newly arriving macrophages have a more pro-inflammatory phenotype in the elderly that is reduced under the effect of anti-inflammatory mediators, rate ι_2 (De Maeyer *et al.,* 2021). Vitamin D impairs the activation of macrophages as an increase in VDR expression downregulates the pro-inflammatory cytokines. The equation for M is thus

$$\frac{dM}{dt} = \iota_1 C - \iota_2 GM - \iota_3 M. \tag{2.20}$$

T and B cells. Naive T cells differentiate into the subpopulations, regulatory T cells (Tregs) and Th (consisting of Th17, Th1 and Th2) cells, favouring the development of Tregs in the presence of VDR. Commensal bacteria and probiotics also promote Tregs differentiation but, conversely, pathogenic bacteria downregulate Tregs (Yamamoto & Jørgensen, 2020).

TABLE 4 *Definition, baseline values and units for the epithelial barrier model parameters.*

Parameter	Description	Value	Units
ϵ_1	Proliferation rate of intestinal epithelial cells	4.9×10^{-13}	$(\text{ng.day})^{-1}$
ϵ_2	Rate of repair of damaged epithelial cells by VDR	2×10^{9}	ml/(ng.day)
ϵ_3	Removal rate of damaged epithelial cells by macrophages	3.17×10^{-6}	ml/day
ϵ_4	Damage to epithelial cells by pro-inflammatory mediators	2.7×10^{3}	ml/(ng.day)
ϵ_5	Damage to epithelial cells by pathogenic bacteria	1×10^{-12}	$(\text{CFU.day})^{-1}$

B cells are, like T cells, part of the adaptive immune response. They are in the blood and lymph nodes, as well as in the intestinal mucosa. B cells differentiate into several subpopulations: of interest here are the plasma B cells, which produce IgA, and regulatory B cells Bregs, which, like Tregs, dampen down the immune response (Yamamoto & Jørgensen, 2020). Specific probiotics can also affect differentiation (Cristofori *et al.*, 2021) but we do not consider this mechanism here. We combine Tregs and Bregs into one variable denoted by R that satisfies the equation

$$\frac{dR}{dt} = \frac{(\iota_4 V_{D_a} + \iota_5 F)}{1 + \iota_6 P} - \iota_7 R, \tag{2.21}$$

where ι_4 and ι_5 denote the rates that T cells and B cells differentiate into regulatory T and B cells in the presence of VDR and commensal bacteria, respectively. ι_6 is the rate at which differentiation into regulatory cells is inhibited by pathogenic bacteria and ι_7 is their combined natural death rate.

Antigen-specific T cells proliferate and are activated at the site of contact in response to pathogenic bacteria (rate ι_{10}) and high concentrations of pro-inflammatory cytokines (rate ι_9). They also utilize metabolites for proliferation (rate ι_8). However, VDR, probiotics and commensal bacteria can inhibit T cell proliferation and pro-inflammatory cytokine production. Hence

$$\frac{dT_h}{dt} = \frac{(\iota_8 N_{mb} + \iota_9 C + \iota_{10} P)}{(1 + \iota_{11} V_{D_a} + \iota_{12} F)} - \iota_{13} T_h, \tag{2.22}$$

where ι_{13} is the natural death rates of T_h cells.

B cells are activated at rate ι_{14} by taking up bacterial products (metabolites). Th cells make pro-inflammatory cytokines to help B cells mature (rate ι_{15}) to make antibodies, specifically IgA. Vitamin D impairs the activation of macrophages and B cells (rate ι_{16}) and low serum levels of 25(OH)D have been shown to be inversely correlated with IgA (Yamamoto & Jørgensen, 2020). The equation governing plasma B cells is thus

$$\frac{dB}{dt} = \frac{\iota_{14} N_{mb} + \iota_{15} C}{1 + \iota_{16} V_{D_a}} - \iota_{17} B, \tag{2.23}$$

where ι_{17} is the natural death rates of B cells.

Pro- and anti-inflammatory mediators. VDR expression upregulates anti-inflammatory cytokines produced by epithelial cells at rate α_1 (Abboud *et al.*, 2020). Commensal bacteria stimulate anti-inflammatory cytokine production by regulatory T and B cells at rate α_2. Macrophages also produce anti-inflammatory cytokines after consuming damaged epithelial cells (rate α_3) and pathogens (rate α_4)

TABLE 5 *Definition, baseline values and units for the immune response model parameters.*

Parameter	Description	Value	Units
ι_1	Rate of activation of macrophages by pro-inflammatory cytokines	1.35×10^{9}	$(\text{ng.day})^{-1}$
ι_2	Rate of inhibition of macrophages by anti-inflammatory cytokines	1.13×10^{2}	ml/(ng.day)
ι_3	Natural death rate of macrophages	1	day^{-1}
ι_4	Rate that T/B cells are differentiated into T/B regulatory cells in presence of VDR	2.38×10^{11}	$(\text{ng.day})^{-1}$
ι_5	Rate that T/B cells are differentiated into T/B regulatory cells in presence of commensal bacteria	8.5×10^{-11}	$(\text{CFU.ml.day})^{-1}$
ι_6	Rate at which differentiation into regulatory cells is inhibited by pathogenic bacteria	1×10^{-14}	CFU^{-1}
ι_7	Combined natural death rate of T/B regulatory cells	1	day^{-1}
ι_8	Rate of utilization of metabolites for T-helper cell proliferation	2.57×10^{-8}	$(\text{ng.ml.day})^{-1}$
ι_9	Rate of T-helper cell proliferation in response to pro-inflammatory cytokines	1.12×10^{9}	$(\text{ng.day})^{-1}$
ι_{10}	Rate of T-helper cell proliferation in response to pathogenic bacteria	1.05×10^{-7}	$(\text{CFU.ml.day})^{-1}$
ι_{11}	Rate of inhibition to T helper cell proliferation by VDR	4×10^{6}	ml/ng
ι_{12}	Rate of inhibition to T helper cell proliferation by commensals	1×10^{-15}	CFU^{-1}
ι_{13}	Natural rate of T-helper cell death	10	day^{-1}
ι_{14}	Rate of activation of plasma B cells by bacterial products	1.28×10^{-8}	$(\text{ng.ml.day})^{-1}$
ι_{15}	Rate of maturation of plasma B cells in presence of pro-inflammatory cytokines	5×10^{8}	$(\text{ng.day})^{-1}$
ι_{16}	Rate of inhibition of plasma B cells by VDR	4×10^{8}	ml/ng
ι_{17}	Natural death rate of plasma B cells	0.81	day^{-1}
α_1	Production rate of anti-inflammatory cytokines by epithelial cells upregulated by VDR	7.08×10^{5}	day^{-1}
α_2	Production rate of anti-inflammatory cytokines by T and B regulatory cells stimulated by commensal bacteria	2.07×10^{-21}	ng/(CFU.day)
α_3	Production rate of anti-inflammatory cytokines by macrophages after consuming damaged epithelial cells	1.13×10^{-7}	ng/day
α_4	Production rate of anti-inflammatory cytokines by macrophages after consuming pathogenic bacteria	1.69×10^{-20}	ng/(CFU.day)
α_5	Natural degradation rate of anti-inflammatory cytokines	7.5×10^{2}	day^{-1}
α_6	Production rate of pro-inflammatory cytokines in response to damaged epithelial cells	9.3×10^{-18}	ng/(CFU.ml.day)
α_7	Production rate of pro-inflammatory cytokines by activated innate immune cells	5.94×10^{-11}	ng/day
α_8	Inhibition of pro-inflammatory cytokines by VDR	4×10^{7}	ml/ng
α_9	Inhibition of pro-inflammatory cytokines by commensals	5×10^{-15}	CFU^{-1}
α_{10}	Production rate of pro-inflammatory cytokines by T helper cells	8.78×10^{-24}	ng/(CFU.day)
α_{11}	Natural degradation rate of pro-inflammatory cytokines	1.2	day^{-1}
α_c	Rate of pro-inflammatory cytokine release by damaged epithelial cells	2.3×10^{-3}	ng/(ml.day)
α_g	Rate of anti-inflammatory cytokine release by healthy epithelial cells	1.77×10^{-3}	ng/(ml.day)
γ_c	Background production rate of pro-inflammatory cytokines	3.24×10^{-4}	ng/(ml.day)
γ_g	Background production rate of anti-inflammatory cytokines	0.35	ng/(ml.day)

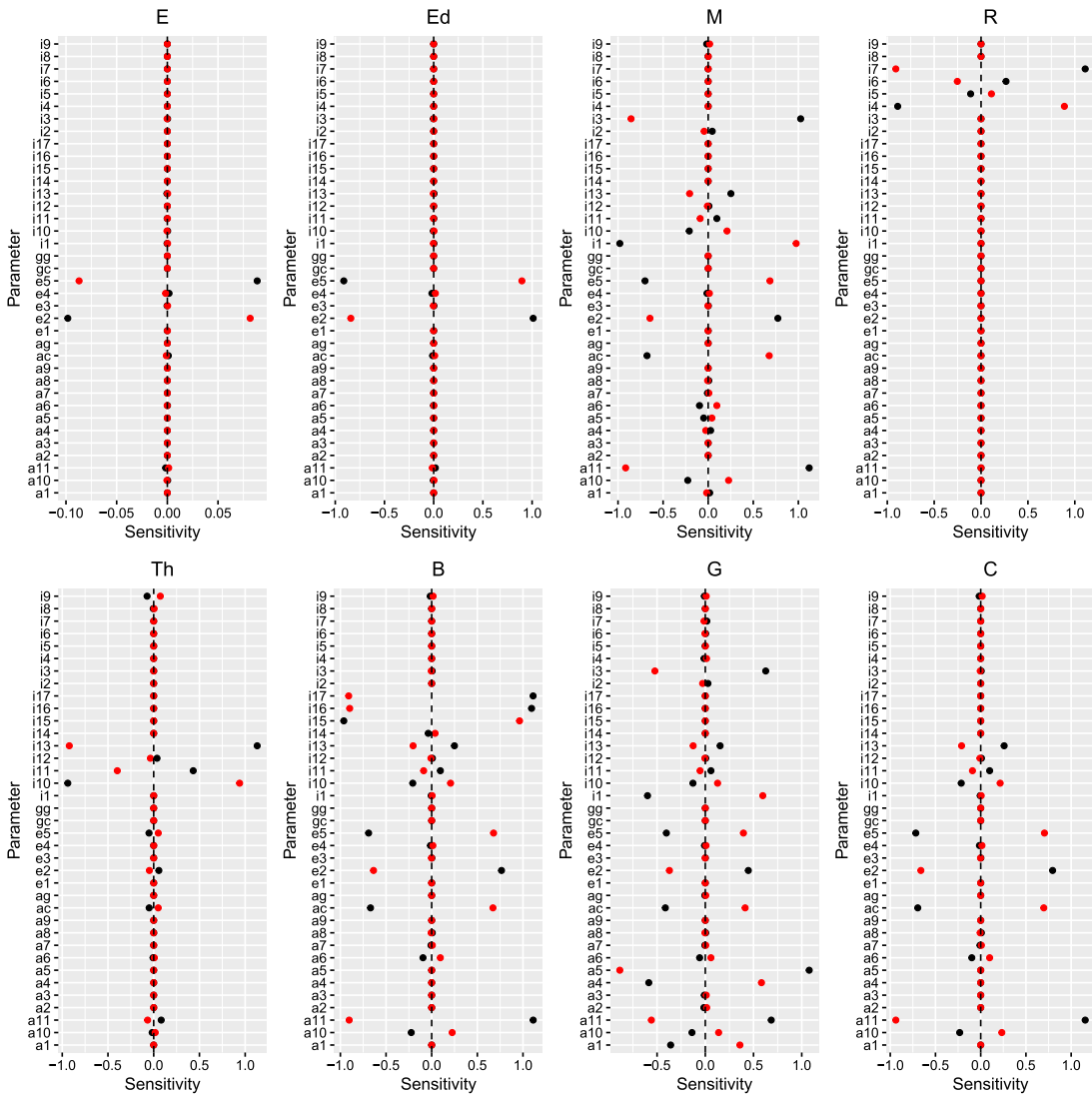

FIG. 11. The effect of varying parameter values on the steady state volume fractions of healthy and damaged epithelial cells, densities of macrophages, regulatory cells and plasma B cells and concentrations of anti- and pro-inflammatory cytokines. Baseline parameter values are taken from Tables 4 and 5 and each parameter is sequentially varied by a 10% decrease (black) and a 10% increase (red). Sensitivity is defined by equation (2.8). We assume that the pathogenic population $P = 3.5 \times 10^{13}$ CFU, VDR complex $V_{D_a} = 1.83 \times 10^{-7}$ ng/ml, commensal population $F = 6.4 \times 10^{13}$ CFU and concentration of metabolites $N_{mb} = 768$ g. Note that i=ι, a=α, e=ϵ and g=γ.

(Yamamoto & Jørgensen, 2020). The dynamics of the anti-inflammatory cytokines is then

$$\frac{dG}{dt} = \gamma_g + (\alpha_g + \alpha_1 V_{D_a})E + \alpha_2 FR + (\alpha_3 E_d + \alpha_4 P)M - \alpha_5 G, \tag{2.24}$$

where α_5 is the natural degradation rate and intestinal epithelial cells release anti-inflammatory cytokines at a low-level background rate α_g. γ_g represents the background production of anti-inflammatory cytokines by other cells.

Pro-inflammatory cytokines are released when the epithelial cells are stressed (due to pathogenic bacteria at rate $\alpha_6 E_d P$). VDR reduces pro-inflammatory cytokines (rate α_8) and it has been shown that a deficiency of VDR expression in macrophages and granulocytes results in an increase in pro-inflammatory cytokines (Nielsen *et al.,* 2018). Further production of pro-inflammatory cytokines is carried out by activated innate immune cells (rate α_7) and by Th cells in response to the pathogenic bacteria (rate α_{10}). Commensal bacteria lead to a downregulation of pro-inflammatory cytokine production by macrophages, rate α_9. Regulatory cells also dampen down their production by increasing the concentration of anti-inflammatory cytokines that decrease the macrophage density (Yamamoto & Jørgensen, 2020). Hence

$$\frac{dC}{dt} = \gamma_c + (\alpha_c + \alpha_6 P)E_d + \frac{\alpha_7 M}{(1 + \alpha_8 V_{D_a} + \alpha_9 F)} + \alpha_{10} P T_h - \alpha_{11} C, \tag{2.25}$$

where α_{11} is the natural pro-inflammatory cytokine decay rate and damaged intestinal epithelial cells release pro-inflammatory cytokines at a low-level background rate α_c. γ_c represents the background production of pro-inflammatory cytokines by other cells.

We assume initially, at time $t = 0$, that the epithelial barrier is healthy and the density of immune cells is at steady state:

$$E_0 = 1, \quad E_{d_0} = 0, \quad M_0 = M_{ss}, \quad R_0 = R_{ss}, \quad T_{h_0} = T_{h_{ss}}, \quad B_0 = B_{ss}, \quad G_0 = G_{ss}, \quad C_0 = C_{ss}. \tag{2.26}$$

where subscript $_{ss}$ denotes the immune cell densities at steady state.

2.3.1 *Parameter values and sensitivity for immune response model.* All the parameters in this sub-model are unknown but estimates are given in Tables 4 and 5.

Given the lack of information on the parameters, the sensitivity analysis is particularly important for this sub-model. We use constant values for the bacterial populations F and P, the concentration of metabolites N_{mb} and the concentration of the VDR:1,25$(OH)_2$D complex V_{D_a} and implement a similar method to that described in Subsection 2.1.1 to assess the sensitivity of the model to local changes in the baseline parameters given in Tables 4 and 5. The sensitivity plots are presented in Fig. 11.

The volume fraction of healthy and damaged epithelial cells is sensitive to the rates of repair of damaged epithelial cells by VDR and of damage to epithelial cells by pathogenic bacteria, ϵ_2 and ϵ_5, respectively. These two parameters also influence the density of macrophages and plasma B cells and the concentration of anti- and pro-inflammatory cytokines, along with the natural degradation of pro-inflammatory cytokines α_{11} and the rate of pro-inflammatory cytokine release by damaged epithelial cells α_c. A decrease in the death rate of macrophages ι_3 and an increase in the rate of activation of macrophages by pro-inflammatory cytokines ι_1 results in an increase in macrophages and anti-inflammatory cytokines. The latter is also influenced by its production rate by macrophages after consuming pathogenic bacteria α_4 and the rate that T and B cells are differentiated into regulatory cells in the presence of commensal bacteria ι_5. Also of note is the sensitivity of plasma B cells to their rate of maturation in the presence of pro-inflammatory cytokines ι_{15}, the rate of their inhibition by VDR ι_{16} and their natural death rate ι_{17}. Regulatory cells are sensitive to a decrease in their death rate ι_7 and changes to the rate of their production in the presence of VDR ι_4. Finally, a decrease in the rates of inhibition to Th

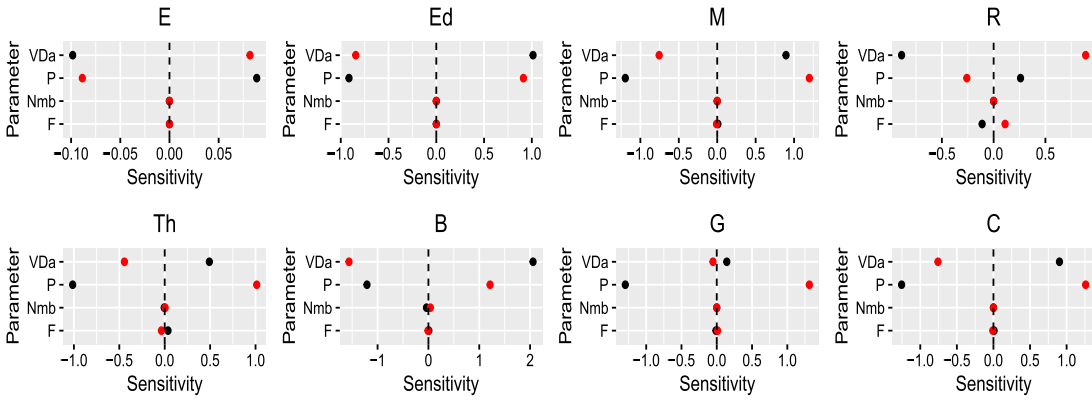

FIG. 12. The effect of varying parameter values on the steady state volume fractions of healthy and damaged epithelial cells, densities of immune cells and concentrations of pro and anti-inflammatory mediators. Baseline parameter values are taken from Tables 4 and 5 with N_{mb} and V_{D_a} sequentially varied by a 10% decrease (black) and a 10% increase (red). F and P are sequentially varied by a 1% decrease (black) and a 1% increase (red). Sensitivity is defined by equation (2.8).

cell proliferation by VDR ι_{11} and natural death of Th cells ι_{13} and an increase in the rate of Th cell proliferation in response to pro-inflammatory cytokines ι_{10} results in an increase in the density of Th cells.

The sensitivity of the model to the variables N_{mb}, F, P and V_{D_a} is shown in Fig. 12. To ensure that the total population of bacteria ($F+P$) does not exceed its maximum value of 1×10^{14} we consider a 1% change in F and P. All variables are sensitive to a change in the concentration of the VDR:1,25(OH)$_2$D complex, particularly plasma B cells (2-fold change). An increase in the population of pathogenic bacteria results in a decrease of healthy epithelial and regulatory cells and an upregulation of damaged epithelial cells, macrophages, Th cells, plasma B cells and cytokines. The density of regulatory cells increases or decreases with corresponding changes to commensal bacteria.

The steady state volume fractions of epithelial cells, immune cell densities and cytokine concentrations are not influenced by changes in the initial conditions.

2.3.2 *Model results for immune response.* We solve equations (2.18)–(2.25) using the parameter values in Tables 4 and 5 to predict the time evolution of epithelial cells, immune cells and inflammatory mediators. We assume constant values for the commensal and pathogenic bacteria and the concentrations of metabolites and of the VDR:1,25(OH)$_2$D complex, based on the steady state values predicted in the previous two sections with and without inflammation.

Figure 13 illustrates the dependence of the epithelial and immune cells on the concentration of metabolites, populations of bacteria and the VDR:1,25(OH)$_2$D complex. As N_{mb} decreases, the volume fraction of healthy epithelial cells very quickly decreases as metabolites provide energy for their proliferation. This results in an increase in damaged epithelial cells that are under stress, increasing signalling of pro-inflammatory cytokines that upregulate the density of macrophages, Th and plasma B cells. The concentration of anti-inflammatory cytokines also increases as they attempt to counteract the effects of the pro-inflammatory mediators. The density of regulatory cells decreases as pathogenic bacteria downregulate their production.

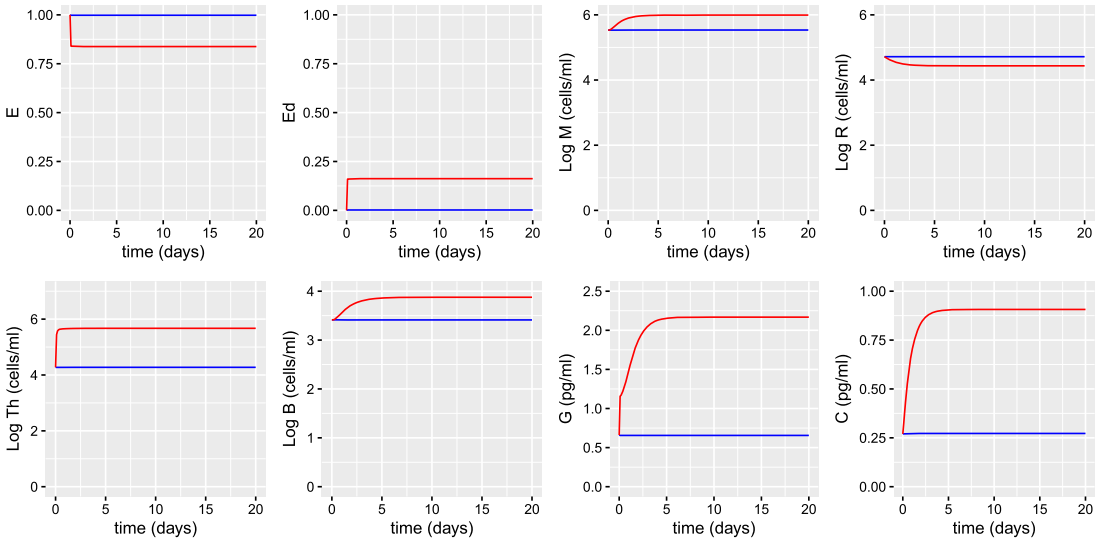

FIG. 13. Simulations predicting the volume fraction of healthy E and damaged epithelial cells E_d, the densities of macrophages M, regulatory cells R, Th cells T_h and plasma B cells B and the concentrations of anti- and pro-inflammatory cytokines, G and C, from solving equations (2.18)–(2.25) with baseline parameters given in Tables 4 and 5. Values for V_{D_a}, N_{mb}, F and P have been taken from the steady state solutions with and without inflammation predicted in Figs 6 and 9 i.e. $V_{D_a} = 1.83 \times 10^{-7}$ ng/ml, $N_{mb} = 1530$ g, $F = 9.94 \times 10^{13}$ CFU, $P = 9.6 \times 10^{7}$ CFU (blue) and $V_{D_a} = 1.83 \times 10^{-7}$ ng/ml, $N_{mb} = 3.4$ g, $F = 3 \times 10^{13}$ CFU, $P = 6.9 \times 10^{13}$ CFU (red).

2.4 *Sensitivity analysis for integrated model*

The three models described by equations (2.1)–(2.26) are now combined so that quantities treated as constant in the sub-models, now vary and are determined from their ODE. A similar method to that described in Subsection 2.1.1 is used to assess the sensitivity of the integrated model. Sensitivity plots for the bacterial populations, VDR:1,25(OH)$_2$D complex, volume fraction of healthy epithelial cells and concentration of pro-inflammatory cytokines are presented in Figs A31–A33 in Appendix A.

Sensitivity of the model to local changes in the baseline parameters given in Tables 2–5 indicates that the parameters influencing the bacterial populations, concentrations of nutrients, concentrations of 25(OH)D and its metabolites, volume fractions of healthy and damaged epithelial cells, densities of immune cells and cytokine concentrations are the same as for the individual sub-models described in subsections 2.1.1, 2.2.1 and 2.3.1. However, the volume fraction of healthy and damaged epithelial cells, densities of immune cells and cytokine concentrations are additionally dependent upon parameters influencing the populations of pathogenic bacteria and the VDR:1,25(OH)$_2$D complex. This is consistent with the sensitivity analysis performed in Fig. 12 for the immune sub-model, which showed that the immune variables had a high dependence on P and V_{D_a}. Figure A32 suggests that the commensal and pathogenic bacterial populations, concentrations of VDR:1,25(OH)$_2$D and pro-inflammatory cytokines and volume fraction of healthy epithelial cells are insensitive to small doses of probiotics. Similarly, the bacterial populations are not influenced by low levels of vitamin D supplementation. However, an increase in vitamin D intake results in an increase in VDR:1,25(OH)$_2$D and healthy epithelial cells and a decrease in pro-inflammatory cytokines, indicating its potential therapeutic benefits.

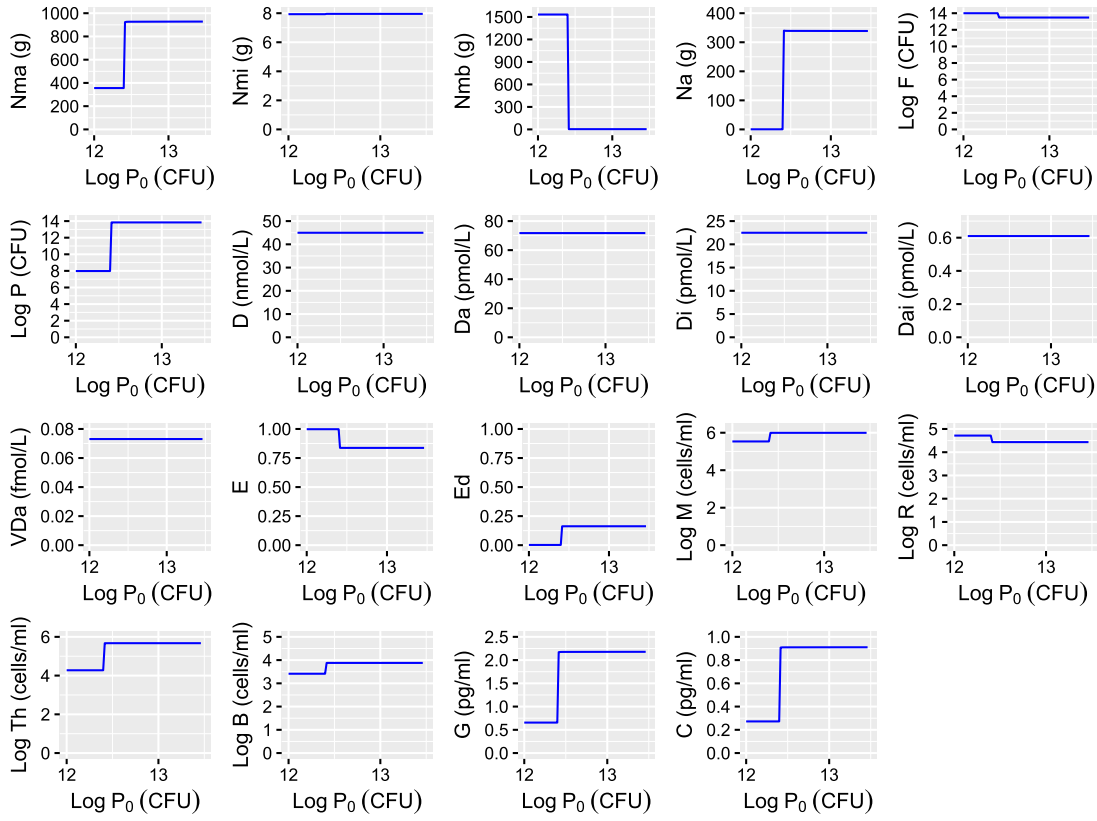

FIG. 14. The predicted steady state concentrations of nutrients, bacterial populations, epithelial cells and immune response from solving equations (2.1)–(2.26) with baseline parameters given in Tables 2–5 with increasing initial pathogen population P_0 and decreasing commensal population F_0. Initial conditions are given by equations (2.7), (2.16) and (2.26) with P_0 increasing from 1×10^{12} to 0.5×10^{14} and F_0 remaining constant at 0.5×10^{14}. Probiotic and vitamin D supplementation is not considered.

The sensitivity of the full model to the initial conditions is also the same as for the individual sub-models, where the steady state values of the model variables are only influenced by changes in the initial pathogen population P_0 (see Fig. 14). As in section 2.1.1, the system is bistable so that when the initial pathogen population exceeds approximately 0.27×10^{13} CFU, it transitions to an inflammatory state resulting in an increase of damaged epithelial cells, signalling of pro-inflammatory cytokines and activation of immune cells.

The predictions for the full model are presented in the following section, where we also explore the effect of supplementation of vitamin D and probiotics on the model variables.

3. Results—integrated model

3.1 *Model results for integrated model—no supplementation*

We solve the full model given by equations (2.1)–(2.26) using the parameter values in Tables 2–5 to predict the time evolution of nutrients and bacteria, vitamin D and its metabolites, epithelial cells,

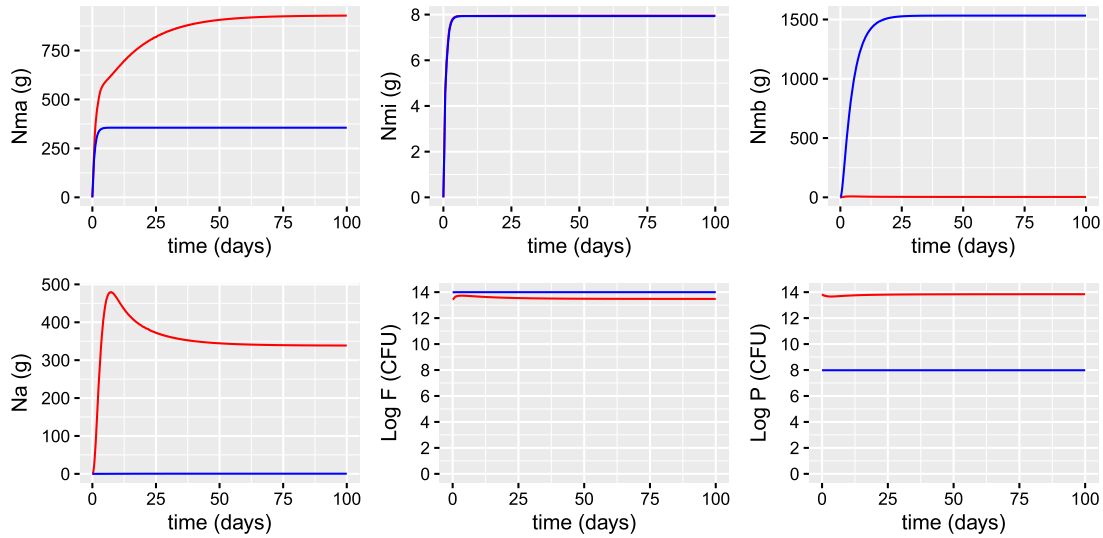

FIG. 15. The predicted concentrations of macronutrients, micronutrients, metabolites, alternate nutrients and populations of commensal and pathogenic bacteria, from solving equations (2.1)–(2.26) with baseline parameters given in Tables 2–5 for an individual with normobiosis (blue) and dysbiosis (red). Initial conditions are given by equations (2.7), (2.16) and (2.26) but in the dysbiosis case, the initial populations of commensal and pathogenic bacteria are altered so that $F_0 = 2.86 \times 10^{13}$ and $P_0 = 7.07 \times 10^{13}$ at $t = 0$. These values have been taken from the inflammatory case in Fig. 6. Probiotic and vitamin D supplementation is not considered.

immune cells and inflammatory mediators under normobiosis and dysbiosis. We assume that dysbiosis is caused by an imbalance in bacterial composition and simulate this by changing the initial composition of commensal and pathogenic bacteria based on the steady state solutions predicted for the inflammatory case in Fig. 6. Initial conditions for the remaining variables do not change. A comparison between the predicted values of the model variables for the two scenarios is presented in Figs 15–17.

Model predictions are similar to those obtained for the individual sub-models with the population of pathogenic bacteria growing under inflammatory conditions, heightening the immune response and causing damage to the host epithelial cells. Pro-inflammatory compounds enhance the production of alternative nutrients (in Fig. 15, N_a at steady state increases from 0.4g to 340g between the non-inflammatory and inflammatory states) that are utilized by the pathogenic bacteria so that they dominate over the commensals. Enhanced production of alternative nutrients is often seen with severe inflammation and may reflect a dysregulated/inappropriate immune response as observed in cytokine storms and sepsis. It is worth noting however, that the upregulated immune response doesn't appear to suppress the pathogen population.

3.2 *Vitamin D supplementation*

Approximately 50% of the global population have insufficient levels of vitamin D (50–75 nmol/L) and around 35% are deficient (<50 nmol/L) (Nair & Maseeh, 2012; Palacios & Gonzalez, 2014). We therefore explore the impact of vitamin D supplementation on individuals with various initial serum 25(OH)D concentrations. Simulation of the same dose of vitamin D (D^0) being given to both vitamin D deficient and sufficient (>75 nmol/L) individuals on the resulting serum levels of 25(OH)D is shown in Fig. 18.

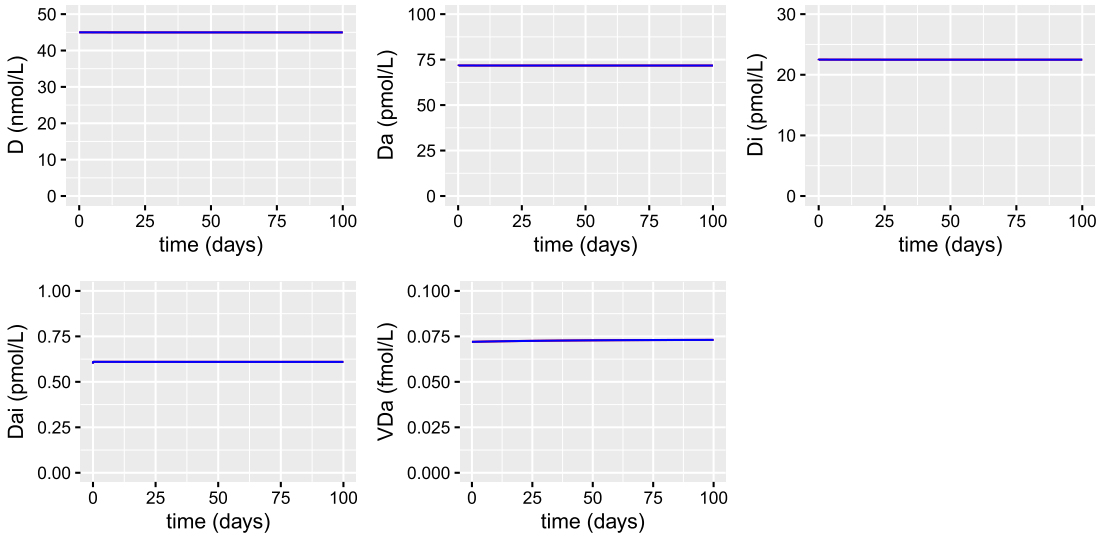

FIG. 16. The predicted time evolution of extracellular and intracellular 25(OH)D and 1,25$(OH)_2$D and the VDR:1,25$(OH)_2$D complex, from solving equations (2.1)–(2.26) with baseline parameters given in Tables 2–5 for an individual with normobiosis (blue) and dysbiosis (red). Initial conditions are given by equations (2.7), (2.16) and (2.26) but in the dysbiosis case, the initial populations of commensal and pathogenic bacteria are altered so that $F_0 = 2.86 \times 10^{13}$ and $P_0 = 7.07 \times 10^{13}$ at $t = 0$. These values have been taken from the inflammatory case in Fig. 6. Probiotic and vitamin D supplementation is not considered.

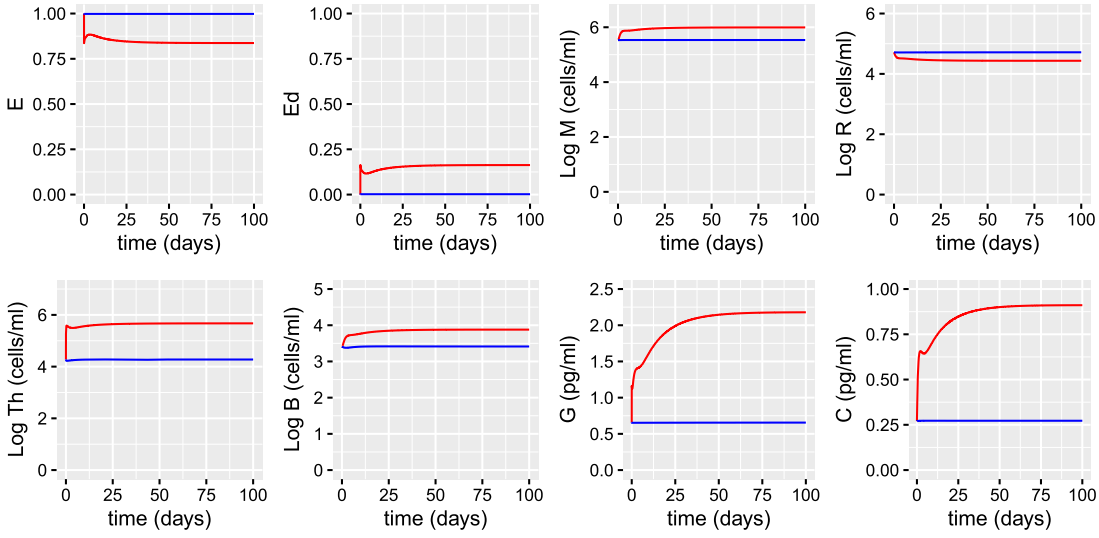

FIG. 17. The predicted volume fraction of healthy and damaged epithelial cells, densities of macrophages, regulatory cells, Th cells and plasma B cells and concentrations of anti- and pro-inflammatory cytokines, from solving equations (2.1)–(2.26) with baseline parameters given in Tables 2–5 for an individual with normobiosis (blue) and dysbiosis (red). Initial conditions are given by equations (2.7), (2.16) and (2.26) but in the dysbiosis case, the initial populations of commensal and pathogenic bacteria are altered so that $F_0 = 2.86 \times 10^{13}$ and $P_0 = 7.07 \times 10^{13}$ at $t = 0$. These values have been taken from the inflammatory case in Fig. 6. Probiotic and vitamin D supplementation is not considered.

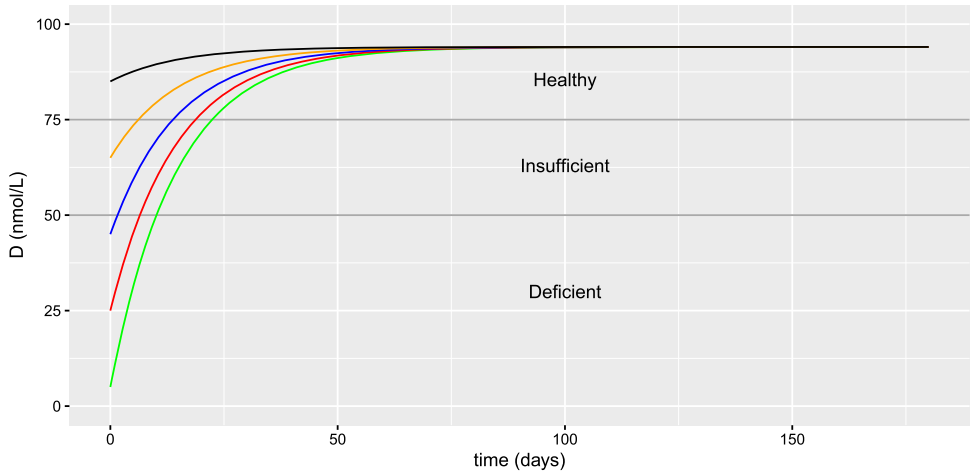

FIG. 18. Simulations predicting the effect of vitamin D supplementation on individuals with varying initial serum concentrations of 25(OH)D solving equations (2.1)–(2.25) with baseline parameters given in Tables 2–5. The initial serum concentrations of 25(OH)D are $D_0 = 5$(green), 25(red), 45(blue), 65(orange) and 85(black) nmol/L and the intake rate $D^0 = 5$ nmol/L day^{-1}.

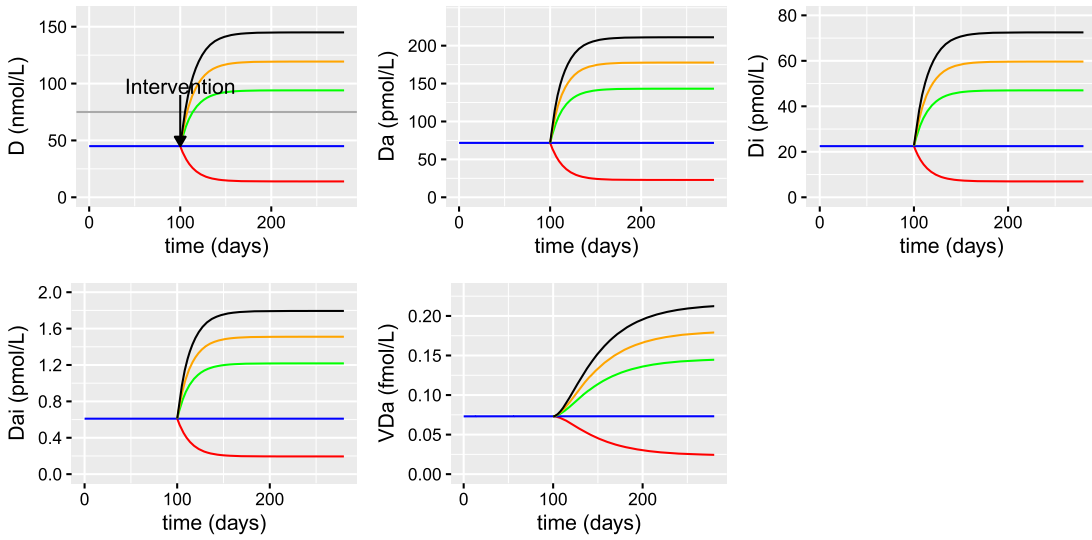

FIG. 19. The predicted time evolution of extracellular and intracellular 25(OH)D and 1,25(OH)$_2$D and the VDR:1,25(OH)$_2$D complex with increasing vitamin D intake from solving equations (2.1)–(2.25) with baseline parameters given in Tables 2–5. Initial conditions are assumed to be the steady state values predicted in Figs 15–17 for the dysbiosis case. A daily intervention of vitamin D supplements is administered from day 100. Simulations represent reduced intake of vitamin D ($D^0 = 1$ nmol/L day^{-1}) (red), no supplementation ($D^0 = 3.2$ nmol/L day^{-1}) (blue), supplementation of 10 μg/day of 25(OH)D ($D^0 = 6.5$ nmol/L day^{-1}) (green), 15 μg/day ($D^0 = 8.3$ nmol/L day^{-1}) (orange) and 20 μg/day ($D^0 = 10$ nmol/L day^{-1}) (black).

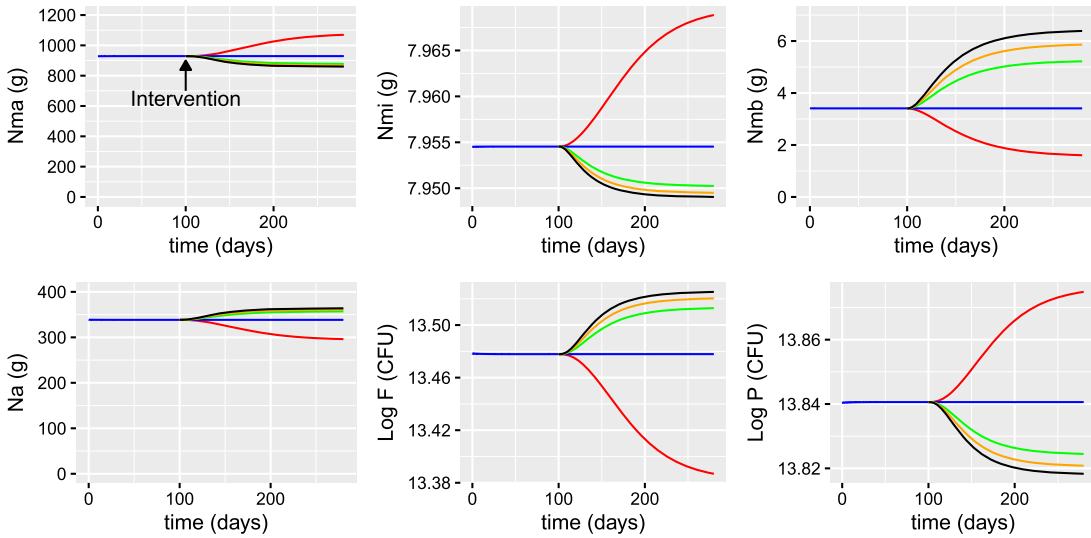

FIG. 20. The predicted concentrations of macronutrients, micronutrients, metabolites, alternate nutrients and populations of commensal and pathogenic bacteria with increasing vitamin D intake from solving equations (2.1)–(2.25) with baseline parameters given in Tables 2–5. Initial conditions are assumed to be the steady state values predicted in Figs 15–17 for the dysbiosis case. A daily intervention of vitamin D supplements is administered from day 100. Simulations represent reduced intake of vitamin D ($D^0 = 1$ nmol/L day^{-1}) (red), no supplementation ($D^0 = 3.2$ nmol/L day^{-1}) (blue), supplementation of 10 μg/day of 25(OH)D ($D^0 = 6.5$ nmol/L day^{-1}) (green), 15 μg/day ($D^0 = 8.3$ nmol/L day^{-1}) (orange) and 20 μg/day ($D^0 = 10$ nmol/L day^{-1}) (black). Note the magnified scale of the vertical axes for N_{mi}, Log F and Log P in order to observe more clearly the effect of supplementation on these variables.

All individuals eventually attain the same steady state concentration of serum 25(OH)D following supplementation, but the most deficient individuals take longer to achieve this concentration. Supplementation therefore has less of an effect on healthy individuals and the simulation suggests that those that are deficient need to take supplements for longer to have the greatest benefit.

We now examine the effect of changing the dose of vitamin D, D^0, on a deficient individual with levels of inflammation predicted in Figs 15–17 for dysbiosis. Simulations of the serum levels of 25(OH)D and its metabolites with supplementation corresponding to 10–20μg/day, no supplementation and a reduced vitamin D intake are presented in Fig. 19.

The serum levels of 25(OH)D increase approximately linearly with vitamin D intake, reaching a maximum steady state concentration following a constant daily dose at around 80 days. When intake of vitamin D is too low, levels of 25(OH)D decrease, so that the individual becomes vitamin D deficient. Doses of 10, 15 and 20 μg/day all result in concentrations of 25(OH)D above the healthy serum level (75 nmol/L) thought to be necessary to maximize the effect of vitamin D on calcium, bone and muscle metabolism (Holick *et al.*, 2011; Rosen *et al.*, 2012) and compare favourably with the profile of measured serum vitamin D levels in healthy older adults supplemented with varying doses of vitamin D over six months presented in Fig. 2A in Graeff-Armas *et al.* (2020).

Increasing vitamin D intake also increases extracellular 1,25(OH)$_2$D, intracellular 25(OH)D, intracellular 1,25(OH)$_2$D and the VDR:1,25(OH)$_2$D complex. While we observe a linear relationship between 25(OH)D and 1,25(OH)$_2$D, experimentally Tang *et al.* (2019) did not observe a strong correlation in their serum concentrations despite a direct enzymatic conversion between them. However, as shown

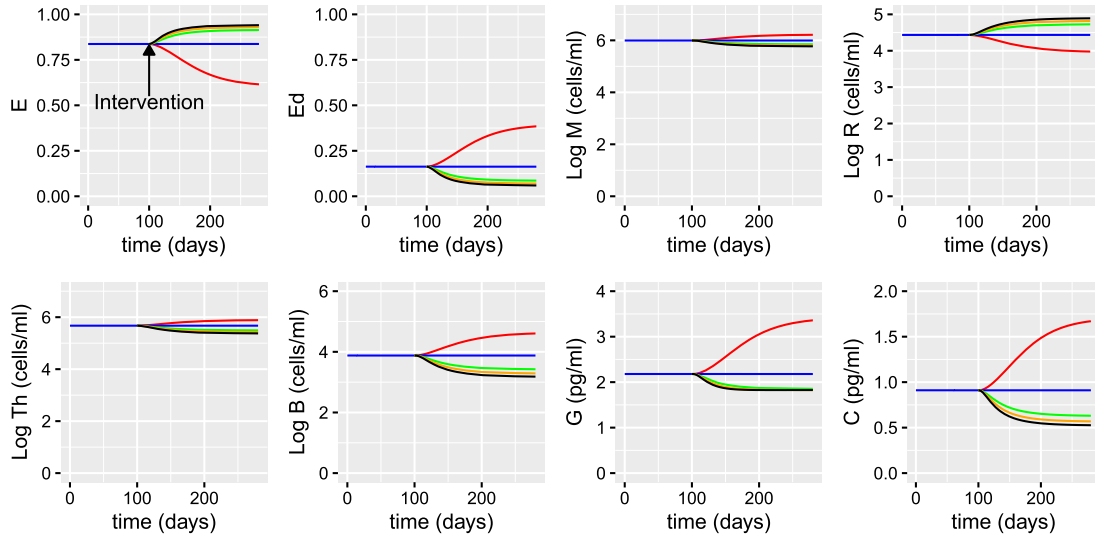

FIG. 21. The predicted volume fraction of healthy and damaged epithelial cells, densities of macrophages, regulatory cells, Th cells and plasma B cells and concentrations of anti- and pro-inflammatory cytokines with increasing vitamin D intake from solving equations (2.1)–(2.25) with baseline parameters given in Tables 2–5. Initial conditions are assumed to be the steady state values predicted in Figs 15–17 for the dysbiosis case. A daily intervention of vitamin D supplements is administered from day 100. Simulations represent reduced intake of vitamin D ($D^0 = 1$ nmol/L day^{-1}) (red), no supplementation ($D^0 = 3.2$ nmol/L day^{-1}) (blue), supplementation of 10 μg/day of 25(OH)D ($D^0 = 6.5$ nmol/L day^{-1}) (green), 15 μg/day ($D^0 = 8.3$ nmol/L day^{-1}) (orange) and 20 μg/day ($D^0 = 10$ nmol/L day^{-1}) (black).

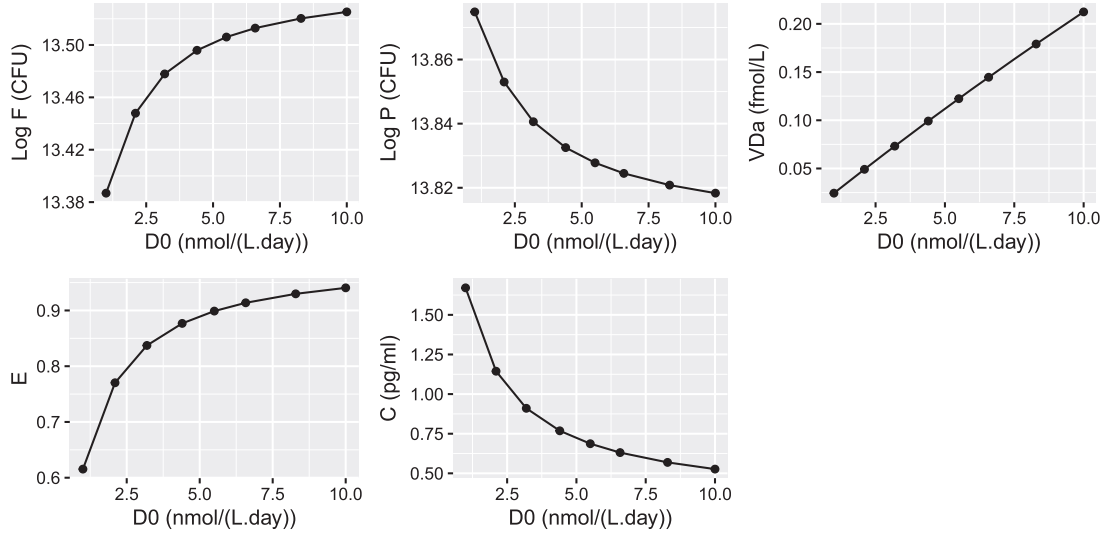

FIG. 22. The predicted populations of commensal and pathogenic bacteria, concentration of VDR:1,25(OH)$_2$D complex, volume fraction of healthy epithelial cells and concentration of pro-inflammatory cytokines on day 180 following daily intervention of vitamin D supplements from day 0 determined from solving equations (2.1)–(2.25) with baseline parameters given in Tables 2–5. Vitamin D intake ranges from $D^0 = 1 - 10$ nmol/L day^{-1} and initial conditions are assumed to be the steady state values predicted in Figs 15–17 for the dysbiosis case.

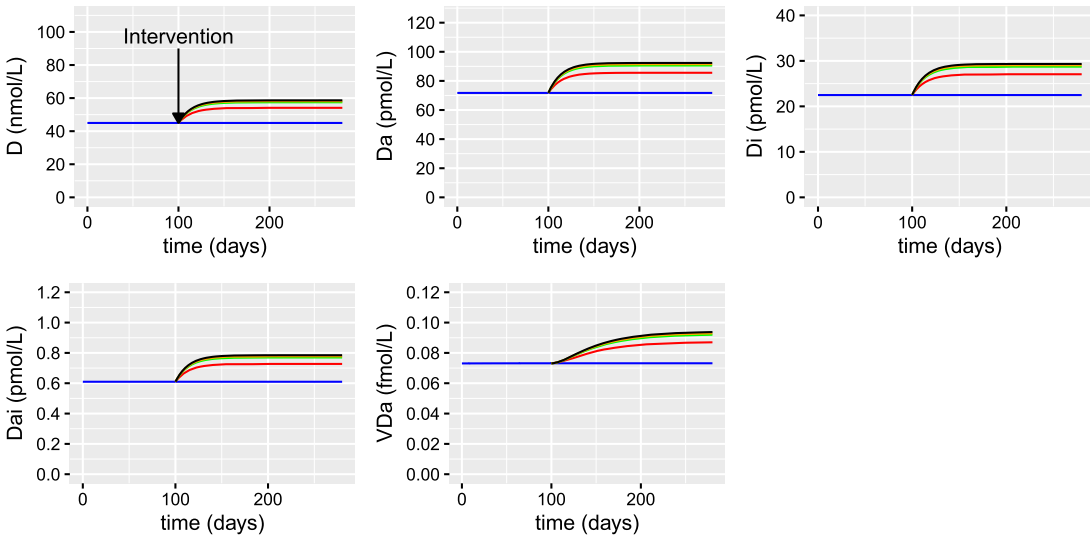

FIG. 23. The predicted concentrations of extracellular and intracellular 25(OH)D and $1,25(OH)_2D$ and VDR:$1,25(OH)_2D$ complex with increasing probiotic intake from solving equations (2.1)–(2.25) with baseline parameters given in Tables 2–5. Initial conditions are assumed to be the steady state values predicted in Figs 15–17 for the dysbiosis case. A daily intervention of probiotic supplements is administered from day 100. Simulations represent no supplements ($P_b = 0$) (blue), $P_b = 1 \times 10^9$ CFU/day (red), 5×10^9 CFU/day (green), 1×10^{10} CFU/day (orange), 1×10^{11} CFU/day (black).

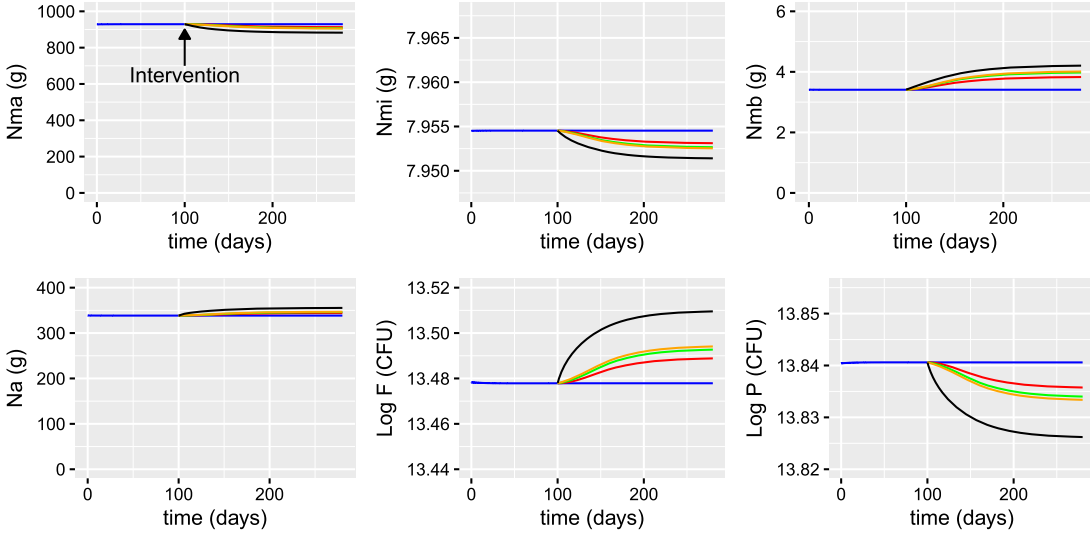

FIG. 24. The predicted concentrations of macronutrients, micronutrients, metabolites, alternate nutrients and populations of commensal and pathogenic bacteria with increasing probiotic intake from solving equations (2.1)–(2.25) with baseline parameters given in Tables 2–5. Initial conditions are assumed to be the steady state values predicted in Figs 15–17 for the dysbiosis case. A daily intervention of probiotic supplements is administered from day 100. Simulations represent no supplements ($P_b = 0$) (blue), $P_b = 1 \times 10^9$ CFU/day (red), 5×10^9 CFU/day (green), 1×10^{10} CFU/day (orange), 1×10^{11} CFU/day (black). Note the magnified scale of the vertical axes for N_{mi}, Log F and Log P in order to observe more clearly the effect of supplementation on these variables.

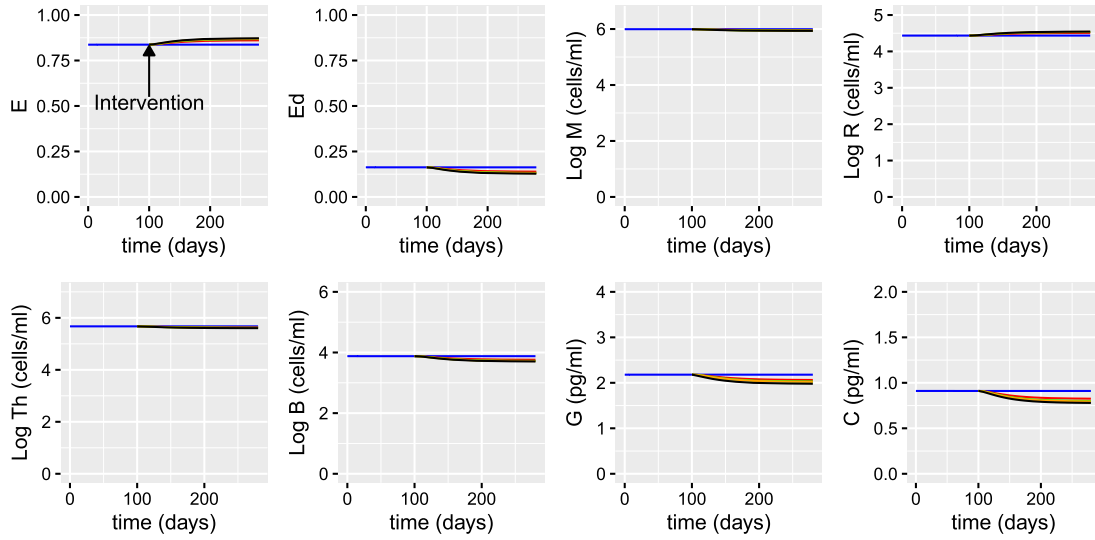

FIG. 25. The predicted volume fraction of healthy and damaged epithelial cells, densities of macrophages, regulatory cells, Th cells and plasma B cells and concentrations of anti- and pro-inflammatory cytokines with increasing probiotic intake from solving equations (2.1)–(2.25) with baseline parameters given in Tables 2–5. Initial conditions are assumed to be the steady state values predicted in Figs 15–17 for the dysbiosis case. A daily intervention of probiotic supplements is administered from day 100. Simulations represent no supplements ($P_b = 0$) (blue), $P_b = 1 \times 10^9$ CFU/day (red), 5×10^9 CFU/day (green), 1×10^{10} CFU/day (orange), 1×10^{11} CFU/day (black).

in Chun *et al.* (2012), Beentjes *et al.* (2019) and Tang *et al.* (2019), there is an upward trend of serum levels of $1,25(OH)_2D$ with increasing serum 25(OH)D and our predictions are within the range observed. The serum and intracellular concentrations of 25(OH)D and $1,25(OH)_2D$ reach a maximum steady state concentration at approximately the same duration after supplementation commences i.e. at 80 days, but the VDR:$1,25(OH)_2D$ complex does not attain steady state until much later, at around 180 days.

Figures 20 and 21 show the nutrient concentrations, bacterial populations, epithelial cells and immune response with increasing vitamin D intake. With no intervention, vitamin D concentrations remain constant and epithelial cells under low-level stress release pro-inflammatory cytokines that stimulate macrophages, plasma B cells and Th cells. When the vitamin D intake is reduced, the vitamin D receptor complex is downregulated, decreasing the density of regulatory cells and increasing the production of pro-inflammatory cytokines by the damaged epithelial cells and hence the densities of macrophages, Th cells and plasma B cells. Anti-inflammatory mediators also increase, dampening down the effect of the inflammatory cytokines. There is small decrease in the concentration of metabolites as more are converted into alternate nutrients by pathogen-induced inflammation.

When vitamin D intake increases, the VDR complex is upregulated, which helps repair the epithelial barrier. An increase in VDR also promotes the development of regulatory cells, inhibits T cell proliferation and pro- and anti-inflammatory cytokine production, impairs the activation of macrophages and B cells and increases the population of commensal bacteria and concentration of metabolites.

Figure 22 shows a summary of the predicted populations of commensal and pathogenic bacteria, concentration of VDR:$1,25(OH)_2D$ complex, volume fraction of healthy epithelial cells and concentration of pro-inflammatory cytokines following the constant daily intervention of vitamin D supplements (intakes ranging from 1–10 nmol/L day^{-1}) for 180 days presented in Figs 19–21. The concentration of

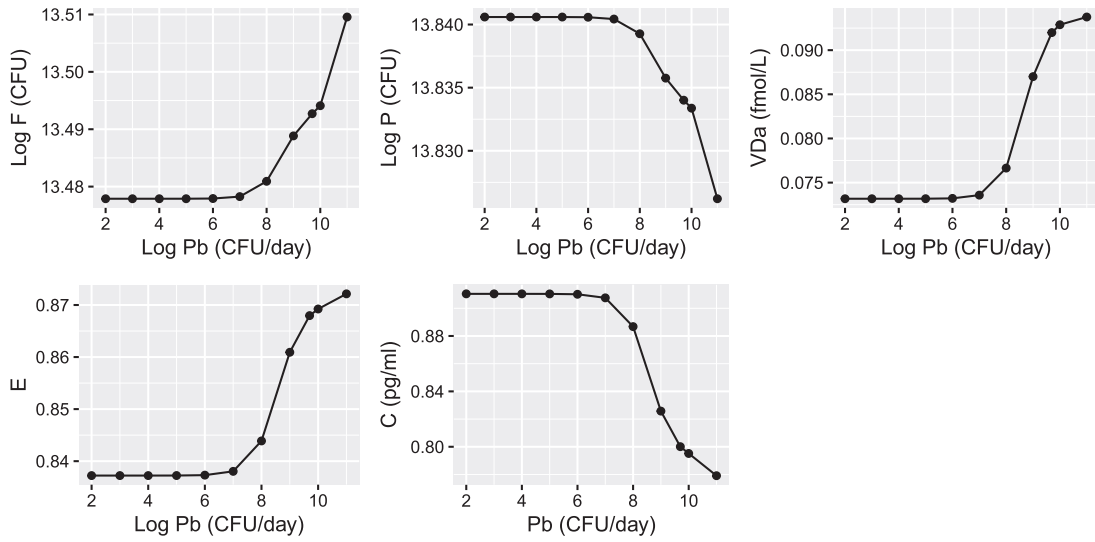

FIG. 26. The predicted populations of commensal and pathogenic bacteria, concentration of VDR:1,25(OH)$_2$D complex, volume fraction of healthy epithelial cells and concentration of pro-inflammatory cytokines on day 180 following daily intervention of probiotic supplements from day 0 determined from solving equations (2.1)–(2.25) with baseline parameters given in Tables 2–5. Probiotic intake ranges from $P_b = 100 - 1 \times 10^{11}$ CFU/day and initial conditions are assumed to be the steady state values predicted in Figs 15–17 for the dysbiosis case.

V_{D_a} increases linearly with vitamin D intake but F, P, E and C all saturate with high doses, indicating that there is a diminishing return on health benefit for higher doses of vitamin D intake.

3.3 *Probiotic supplementation*

The effect of daily administration of probiotics on the model variables is shown in Figs 23–25. Increasing doses of probiotics (P_b) ranging from no supplements to $2\times\ 10^{10}$ CFU/day were given from day 100 without vitamin D supplementation.

Following supplementation, the serum concentration of 25(OH)D and its metabolites increase but this is not a linear effect. Similarly, the increase in healthy epithelial cells and decrease in immune cell density is not linear with probiotic intake. In agreement with Jones *et al.* (2013), serum vitamin D increased by approximately 25% after probiotic administration. As for vitamin D supplementation, the upregulation of the VDR:1,25(OH)$_2$D complex in response to probiotics dampens down inflammation and increases the volume fraction of healthy epithelial and regulatory cells but to a lesser extent than that observed in Fig. 21.

Figure 26 shows a summary of the predicted populations of commensal and pathogenic bacteria, concentration of VDR:1,25(OH)$_2$D complex, volume fraction of healthy epithelial cells and concentration of pro-inflammatory cytokines following the constant daily intervention of probiotic supplements (intakes ranging from 100-1×10^{11} CFU/day) for 180 days presented in Figs 23–25. All variables remain unchanged until the intake of probiotics exceeds approximately 1×10^7 CFU/day when F, V_{D_a} and E start to increase and P and C decrease. E, C and V_{D_a} all saturate with high doses indicating that there is a diminishing improvement in epithelial barrier repair and anti-inflammatory benefits for higher doses

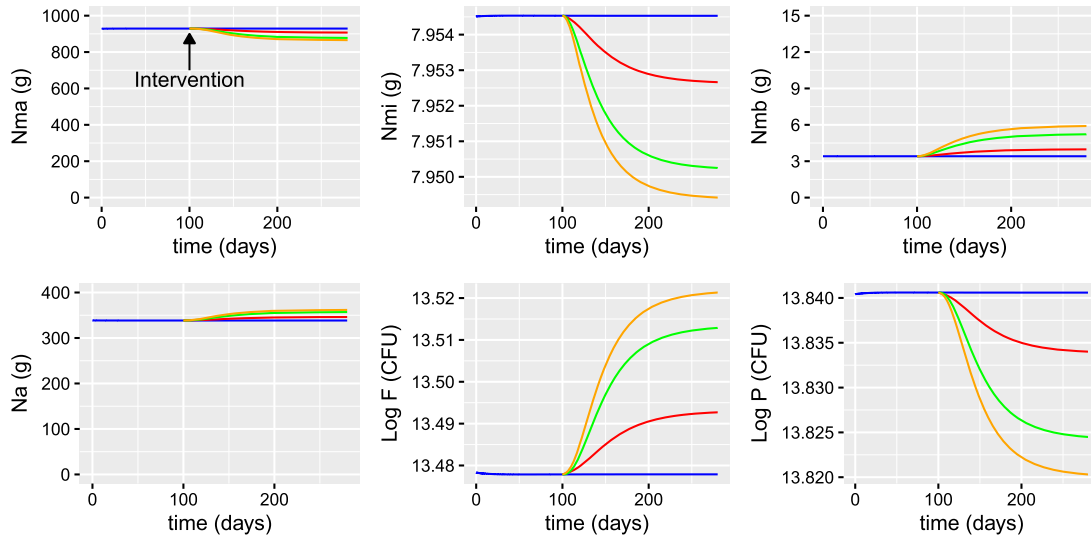

FIG. 27. The predicted concentrations of macronutrients, micronutrients, metabolites, alternate nutrients and populations of commensal and pathogenic bacteria with vitamin D and probiotic co-supplementation from solving equations (2.1)–(2.25) with baseline parameters given in Tables 2–5. Initial conditions are assumed to be the steady state values predicted in Figs 15–17 for the dysbiosis case. A daily intervention is administered from day 100. Simulations represent no supplements ($P_b = 0$, $D^0 = 3.2$ nmol/L day^{-1}) (blue), probiotic supplement only ($P_b = 5 \times 10^9$ CFU/day, $D^0 = 3.2$ nmol/L day^{-1}) (red), vitamin D supplement only ($P_b = 0$, $D^0 = 6.5$ nmol/L day^{-1}) (green) and combined vitamin D and probiotic supplements ($P_b = 5 \times 10^9$ CFU/day, $D^0 = 6.5$ nmol/L day^{-1}) (orange). Note the magnified scale of the vertical axes for N_{mi}, Log F and Log P in order to observe more clearly the effect of supplementation on these variables.

of probiotic intake. However, the bacterial populations continue to increase (commensals) and decrease (pathogens) at high doses.

3.4 *Vitamin D and probiotic supplementation*

Simulations predicting the effect of combining vitamin D and probiotic supplements and comparing levels with those predicted with no supplements, vitamin D only and probiotics only are shown in Figs 27–29. Daily supplements are administered individually or in combination on day 100 and the response of the nutrient concentrations, bacteria populations, levels of vitamin D and its metabolites, volume fraction of epithelial cells and the immune response before and after the intervention are predicted numerically.

As with the individual supplementation described in the previous two subsections, administration of vitamin D and/or probiotic supplements upregulates the vitamin D receptor, which helps repair the epithelial barrier function and stimulates the production of regulatory cells. An increase in macrophages enhances the capacity for VDR:1,25(OH)$_2$D-mediated elimination of pathogenic bacteria, resulting in an upregulation of commensal bacteria and metabolites as more SCFAs are being produced, providing energy for epithelial cell proliferation. Concomitantly, the same VDR:1,25(OH)$_2$D interaction is able to modify antigen-presentation and activated T cell function to promote attenuation of inflammatory T cell responses and enhance tolerogenic regulatory cell activity. In this way vitamin D can act as a double-edged sword within the immune system by enhancing innate antimicrobial immunity, while

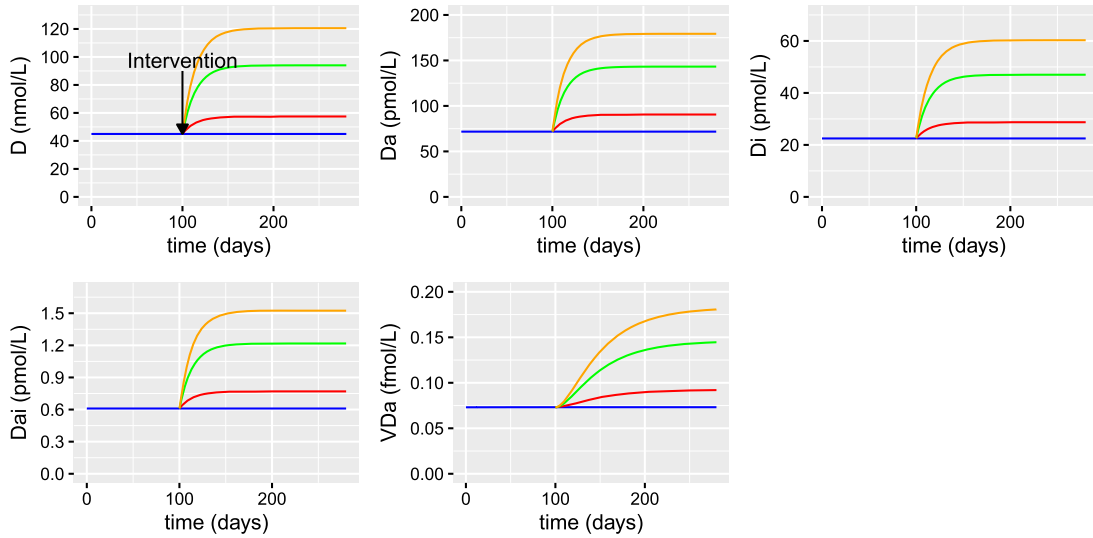

FIG. 28. The predicted concentrations of extracellular and intracellular 25(OH)D and 1,25$(OH)_2$D and VDR:1,25$(OH)_2$D complex with vitamin D and probiotic co-supplementation from solving equations (2.1)–(2.25) with baseline parameters given in Tables 2–5. Initial conditions are assumed to be the steady state values predicted in Figs 15–17 for the dysbiosis case. A daily intervention is administered from day 100. Simulations represent no supplements ($P_b = 0, D^0 = 3.2$ nmol/L day^{-1}) (blue), probiotic supplement only ($P_b = 5 \times 10^9$ CFU/day, $D^0 = 3.2$ nmol/L day^{-1}) (red), vitamin D supplement only ($P_b = 0$, $D^0 = 6.5$ nmol/L day^{-1}) (green) and combined vitamin D and probiotic supplements ($P_b = 5 \times 10^9$ CFU/day, $D^0 = 6.5$ nmol/L day^{-1}) (orange).

simultaneously protecting against potential tissue damage associated with over-exuberant adaptive immunity.

As observed in the individual models, vitamin D supplements enhance the positive effects more than probiotics but taking them in combination results in the greatest benefit. However, co-supplementation produces a combined effect that is less than the sum of the two separate supplements administered individually. This is illustrated more clearly in Fig. 30, where a comparison between the steady states of the metrics F, P, D, V_{D_a}, E and C for the different supplementation regimens is shown.

4. Discussion

Clinical studies examining the possible interactions between vitamin D/VDR pathway and probiotic administration in modulating intestinal inflammation are emerging, and results from initial studies provide a promising therapeutic option for a variety of human diseases (Abboud *et al.,* 2020; Pagnini *et al.,* 2021). The principal aim of this study was to develop a novel mathematical model to describe the possible interactions between probiotics and vitamin D for promoting intestinal homeostasis and immune health.

Mechanistic information and clinical observations from the literature were used to develop the model and inform parameter values where possible. The model simulates the concentration of nutrients in the intestine, populations of commensal and pathogenic bacteria, the concentrations of vitamin D and its metabolites, the volume fractions of healthy and damaged epithelial cells, the densities of immune cells and the concentrations of anti- and pro-inflammatory mediators with and without supplementation. However, the model is sensitive to the choice of parameters and the lack of information

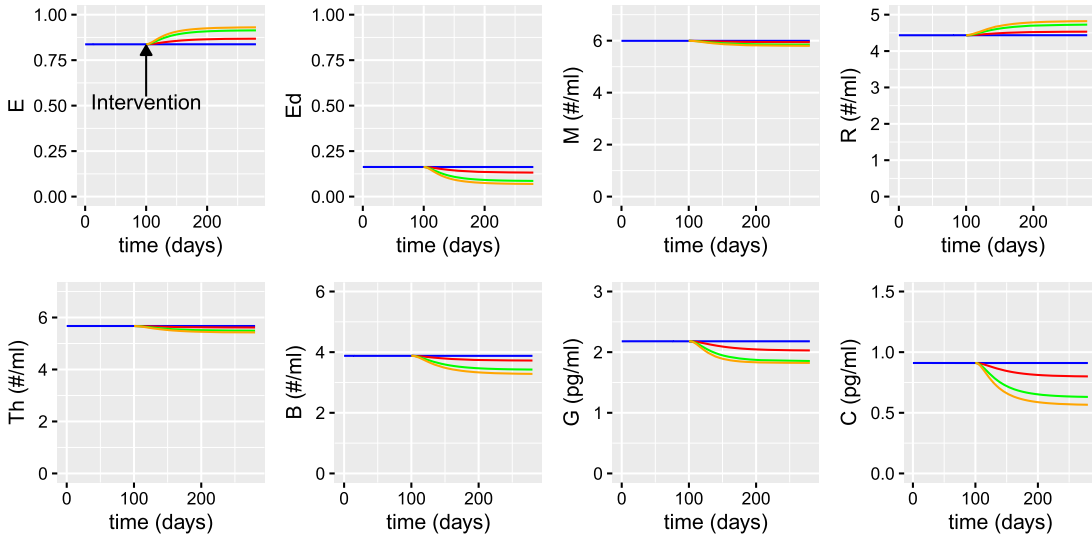

FIG. 29. The predicted volume fractions of healthy and damaged epithelial cells, densities of macrophages, regulatory cells, Th cells and plasma B cells and concentrations of anti- and pro-inflammatory cytokines with vitamin D and probiotic co-supplementation from solving equations (2.1)–(2.25) with baseline parameters given in Tables 2–5. Initial conditions are assumed to be the steady state values predicted in Figs 15–17 for the dysbiosis case. A daily intervention is administered from day 100. Simulations represent no supplements ($P_b = 0$, $D^0 = 3.2$ nmol/L day^{-1}) (blue), probiotic supplement only ($P_b = 5 \times 10^9$ CFU/day, $D^0 = 3.2$ nmol/L day^{-1}) (red), vitamin D supplement only ($P_b = 0$, $D^0 = 6.5$ nmol/L day^{-1}) (green) and combined vitamin D and probiotic supplements ($P_b = 5 \times 10^9$ CFU/day, $D^0 = 6.5$ nmol/L day^{-1}) (orange).

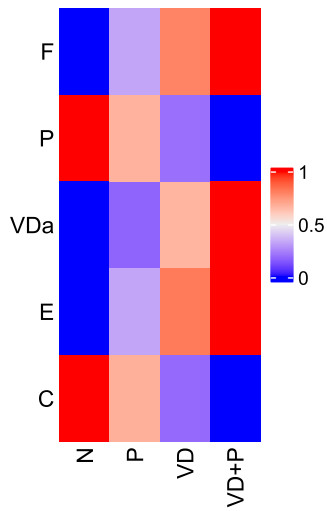

FIG. 30. A comparison summary of the normalized populations of commensal and pathogenic bacteria, concentration of VDR:1.25(OH)$_2$D complex, volume fraction of healthy epithelial cells and concentration of pro-inflammatory cytokines predicted on day 180 following no supplementation (N) and daily interventions of probiotics only (P), vitamin D only (VD) and vitamin D and probiotic co-supplementation (VD+P) from day 0 taken from Figs 27–29.

on certain parameters, particularly in the immune response model, is a limitation of this study. A better understanding of the parameters that govern the bacterial and inflammatory response is essential for more quantitative predictions.

Nevertheless, the parameters have been chosen so that the model is able to predict similar qualitative behaviour to that observed clinically and our attempt to understand the mechanistic interactions between the intestinal microbiota, immune response and vitamin D and probiotic supplementation has highlighted the need for future experimental studies measuring, e.g. the microbiota composition, immune cell phenotypes, inflammatory markers, dietary intake, intestinal barrier integrity markers and markers of vitamin D homeostasis.

Vitamin D levels are low in the UK population (Hyppönen & Power, 2007), and in most other populations, and vitamin D levels among British adults are inversely associated with infection risk (Berry *et al.,* 2011), suggesting that the influence of low vitamin D status on immune competence is a public health problem. Our model has been able to illustrate the potential benefits of supplementation and indicates how the administration of vitamin D supplements to deficient individuals could help them attain the desired vitamin D levels, while suggesting that supplementation has less of an effect on healthy individuals. The model has also predicted that vitamin D supplementation upregulates the VDR complex, which enhances barrier function (and hence increases AMP production by epithelial cells), maintains innate and cell-mediated immunity and prevents low-grade inflammation. In Ogbu *et al.* (2020), it is hypothesized that an upregulation of VDR may increase the commensal production of SFCAs and this proposed behaviour has been captured in our model.

Specific strains of probiotics have different functions and mechanisms of action. They need to survive the passage through the upper gastrointestinal tract and colonize the intestine so that they can affect the immune system positively. By incorporating probiotic supplementation into the input terms in the equations representing the commensal bacteria population and serum concentration of 25(OH)D, our model has suggested that administration of probiotics supports the maintenance of immune cells, enhances intestinal barrier function and protects against intestinal inflammation by mediating inflammatory signalling molecules. The model has also predicted that co-supplementation of vitamin D and probiotics increases the positive effects, as vitamin D intestinal absorption and VDR protein expression are upregulated, enhancing their anti-inflammatory benefits. While there are benefits of combining the two supplements the overall effect is less than the sum of the individual ones and unfortunately, the model does not predict the same synergistic effects of co-supplementation intimated in some studies reviewed by Abboud *et al.* (2020). This indicates that more clinical studies and a greater understanding of the parameters needs to be carried out to clarify the health benefits.

Under inflammatory conditions our model has predicted the loss of intestinal barrier function and growth of the pathogenic bacteria. This can result in the translocation of pathogenic bacteria and their structural components into the bloodstream causing inflammation elsewhere in the body. The structural complexity and functional capability of the intestinal microbiota declines with poor diet and age and is likely a factor causing immunosenescence in older people (Wu *et al.,* 2021). Extending our model to examine these spatial aspects is an interesting area for future study.

The relationship between the intestinal microbiota and human health is an area of increasing interest, and our model, which is parameterized as fully as the available literature allows, is the first to explore the complex interactions between the various mechanistic components and determine the impact of manipulating the intestinal microbiota with dietary components. Despite our many assumptions, the model produces biologically realistic predictions and hence would seem to provide a credible basis for future work in this area.

Acknowledgements

This work was supported by a UKRI Nutrition Research Partnership Award (grant number MR/T001879/1). J.R.K. gratefully acknowledges a Royal Society Leverhulme Trust Senior Fellowship.

References

Abboud, M., Rizk, R., AlAnouti, F., Papandreou, D., Haidar, S. & Mahboub, N. (2020) The Health Effects of Vitamin D and Probiotic Co-Supplementation: A Systematic Review of Randomized Controlled Trials. *Nutrients*, **13**, 111. https://doi.org/10.3390/nu13010111.

Adrian, M. (2020) *Understanding the human gut microbiome: A mathematical approach*. Undergraduate thesis. University of Iowa., https://iro.uiowa.edu/discovery/delivery/01IOWAINST: ResearchRepository/12811139520002771?l13811408760002771.

Bakke, D., Chatterjee, I., Agrawal, A., Dai, Y. & Sun, J. (2018) Regulation of Microbiota by Vitamin D Receptor: A Nuclear Weapon in Metabolic Diseases. *Nucl. Receptor Res.*, **190**, 101377. https://doi.org/10.11131/2018/101377.

Beentjes, C. H. L., Taylor-King, J. P., Bayani, A., Davis, C. N., Dunster, J. L., Jabbari, S., Mirams, G. R., Jenkinson, C., Kilby, M. D., Hewison, M. & Tamblyn, J. A. (2019) Defining vitamin D status using multi-metabolite mathematical modelling: A pregnancy perspective. *J, Steroid Biochem. Mol. Biol*, **190**, 152–160. https://doi.org/10.1016/j.jsbmb.2019.03.024.

Berry, D. J., Hesketh, K., Power, C. & Hyppönen, E. (2011) Vitamin D status has a linear association with seasonal infections and lung function in British adults. *Br. J. Nutr*, **106**, 1433–1440. https://doi.org/10.1017/S0007114511001991.

Bishop, E., Ismailova, A., Dimeloe, S., Hewison, M. & White, J. H. (2020) Vitamin D and Immune Regulation: Antibacterial, Antiviral, Anti-Inflammatory. *JBMR Plus*, **5**, e10405. https://doi.org/10.1002/jbm4.10405.

Chun, R. F., Peercy, B. E., Adams, J. S. & Hewison, M. (2012) Vitamin D binding protein and monocyte response to 25-hydroxyvitamin D and 1,25-dihydroxyvitamin D: analysis by mathematical modeling. *PLoS One.*, **7**, e30773. https://doi.org/10.1371/journal.pone.0030773.

Conlon, M. A. & Bird, A. R. (2014) The impact of diet and lifestyle on gut microbiota and human health. *Nutrients*, **7**, 17–44. https://doi.org/10.3390/nu7010017.

Cristofori, F., Dargenio, V. N., Dargenio, C., Miniello, V. L., Barone, M. & Francavilla, R. (2021) Anti-Inflammatory and Immunomodulatory Effects of Probiotics in Gut Inflammation: A Door to the Body. *Front Immunol*, **12**, –578386. https://doi.org/10.3389/fimmu.2021.578386.

De Maeyer, R. P. H. & Chambers, E. S. (2021) The impact of ageing on monocytes and macrophages. *Immunol. Lett*, **230**, 1–10. https://doi.org/10.1016/j.imlet.2020.12.003.

de Vos, P., Mujagic, Z., de Haan, B. J., Siezen, R. J., Bron, P. A., Meijerink, M., Wells, J. M., Masclee, A. A. M., Boekschoten, M. V., Faas, M. M. & Troost, F. J. (2017) Lactobacillus plantarum Strains Can Enhance Human Mucosal and Systemic Immunity and Prevent Non-steroidal Anti-inflammatory Drug Induced Reduction in T Regulatory Cells. *Front Immunol*, **8**, 1000. https://doi.org/10.3389/fimmu.2017.01000.

Fan, Y. & Pedersen, O. (2021) Gut microbiota in human metabolic health and disease. *Nat. Rev. Microbiol*, **19**, 55–71. https://doi.org/10.1038/s41579-020-0433-9.

Graeff-Armas, L. A., Bendik, I., Kunz, I., Schoop, R., Hull, S. & Beck, M. (2020) Supplemental 25-Hydroxycholecalciferol Is More Effective than Cholecalciferol in Raising Serum 25-Hydroxyvitamin D Concentrations in Older Adults. *J. Nutr*, **150**, 73–81. https://doi.org/10.1093/jn/nxz209.

Hara, A. & Iwasa, Y. (2019) Coupled dynamics of intestinal microbiome and immune system-A mathematical study. *J. Theor. Biol*, **464**, 9–20. https://doi.org/10.1016/j.jtbi.2018.12.021.

Holick, M. F., Binkley, N. C., Bischoff-Ferrari, H. A., Gordon, C. M., Hanley, D. A., Heaney, R. P., Murad, M. H. & Weaver, C. (2011) Evaluation, treatment, and prevention of vitamin D deficiency: an Endocrine Society Clinical Practice Guideline. *J. Clin. Endocrinol. Metab.*, **96**, 1911–1930.

Hyppönen, E. & Power, C. (2007) Hypovitaminosis D in British adults at age 45 y: nationwide cohort study of dietary and lifestyle predictors. *Am. J. Clin. Nutr.*, **85**, 860–868. https://doi.org/10.1093/ajcn/85.3.860.

Jones, M. L., Martoni, C. J. & Prakash, S. (2013) Oral supplementation with probiotic L. reuteri NCIMB 30242 increases mean circulating 25-hydroxyvitamin D: a post hoc analysis of a randomized controlled trial. *J. Clin. Endocrinol. Metab*, **98**, 2944–2951. https://doi.org/10.1210/jc.2012-4262.

Karmali, R., Hewison, M., Rayment, N., Farrow, S. M., Brennan, A., Katz, D. R. & O'Riordan, J. L. (1991) 1,25(OH)2D3 regulates c-myc mRNA levels in tonsillar T lymphocytes. *Immunology*, **74**, 589–593.

Kumar, M., Ji, B., Zengler, K. & Nielsen, J. (2019) Modelling approaches for studying the microbiome. *Nat. Microbiol*, **4**, 1253–1267. https://doi.org/10.1038/s41564-019-0491-9.

Lang, J. M., Eisen, J. A. & Zivkovic, A. M. (2014) The microbes we eat: abundance and taxonomy of microbes consumed in a day's worth of meals for three diet types. *PeerJ*, **2**, e659. https://doi.org/10.7717/peerj.659.

Lopez, D. V., Al-Jaberi, F. A. H., Woetmann, A., Odum, N., Bonefeld, C. M., Kongsbak-Wismann, M. & Geisler, C. (2021) Macrophages Control the Bioavailability of Vitamin D and Vitamin D-Regulated T Cell Responses. *Front. Immunol*, **12**, 722806. https://doi.org/10.3389/fimmu.2021.722806.

Lu, R., Shang, M., Zhang, Y. G., Jiao, Y., Xia, Y., Garrett, S., Bakke, D., Bäuerl, C., Martinez, G. P., Kim, C. H., Kang, S. M. & Sun, J. (2020) Lactic Acid Bacteria Isolated From Korean Kimchi Activate the Vitamin D Receptor-autophagy Signaling Pathways. *Inflamm. Bowel Dis*, **26**, 1199–1211. https://doi.org/10.1093/ibd/izaa049.

Magnúsdóttir, S. & Thiele, I. (2018) Modeling metabolism of the human gut microbiome. *Curr. Opin. Biotechnol*, **51**, 90–96. https://doi.org/10.1016/j.copbio.2017.12.005.

Mujagic, Z., de Vos, P., Boekschoten, M. V., Govers, C., Pieters, H. H., de Wit, N. J., Bron, P. A., Masclee, A. A. & Troost, F. J. (2017) The effects of Lactobacillus plantarum on small intestinal barrier function and mucosal gene transcription; a randomized double-blind placebo controlled trial. *Sci Rep*, **7**, 40128. https://doi.org/10.1038/srep40128.

Nair, R. & Maseeh, A. (2012) Vitamin D: The "sunshine" vitamin. *J. Pharmacol. Pharmacother*, **3**, 118–126. https://doi.org/10.4103/0976-500X.95506.

Nielsen, O. H., Rejnmark, L. & Moss, A. C. (2018) Role of Vitamin D in the Natural History of Inflammatory Bowel Disease. *J. Crohns Colitis*, **12**, 742–752. https://doi.org/10.1093/ecco-jcc/jjy025.

Ogbu, D., Xia, E. & Sun, J. (2020) Gut instincts: vitamin D/vitamin D receptor and microbiome in neurodevelopment disorders. *Open Biol*, **10**, 200063. https://doi.org/10.1098/rsob.200063.

Pagnini, C., Di Paolo, M. C., Graziani, M. G. & Delle Fave, G. (2021) Probiotics and Vitamin D/Vitamin D Receptor Pathway Interaction: Potential Therapeutic Implications in Inflammatory Bowel Disease. *Front Pharmacol*, **12**, 747856. https://doi.org/10.3389/fphar.2021.747856.

Palacios, C. & Gonzalez, L. (2014) Is vitamin D deficiency a major global public health problem? *J. Steroid Biochem. Mol. Biol*., **144** Pt A:138–45. doi: https://doi.org/10.1016/j.jsbmb.2013.11.003.

Pickard, J. M., Zeng, M. Y., Caruso, R. & Núñez, G. (2017) Gut microbiota: Role in pathogen colonization, immune responses, and inflammatory disease. *Immunol. Rev*, **279**, 70–89. https://doi.org/10.1111/imr.12567.

Rosen, C. J., Abrams, S. A., Aloia, J. F., Brannon, P. M., Clinton, S. K., Durazo-Arvizu, R. A., Gallagher, J. C., Gallo, R. L., Jones, G., Kovacs, C. S., Manson, J. E., Mayne, S. T., Ross, A. C., Shapses, S. A. & Taylor, C. L. (2012) IOM committee members respond to Endocrine Society vitamin D guidelines. *J. Clin. Endocrinol. Metab.*, **97**, 1146–1152.

Salazar, N., Arboleya, S., Fernández-Navarro, T., de Los Reyes-Gavilán, C. G., Gonzalez, S. & Gueimonde, M. (2019) Age-Associated Changes in Gut Microbiota and Dietary Components Related with the Immune System in Adulthood and Old Age: A Cross-Sectional Study. *Nutrients*, **11**, 1765. https://doi.org/10.3390/nu11081765.

Sender, R., Fuchs, S. & Milo, R. (2016) Are We Really Vastly Outnumbered? Revisiting the Ratio of Bacterial to Host Cells in Humans. *Cell*, **164**, 337–340. https://doi.org/10.1016/j.cell.2016.01.013.

Shashkova, T., Popenko, A., Tyakht, A., Peskov, K., Kosinsky, Y., Bogolubsky, L., Raigorodskii, A., Ischenko, D., Alexeev, D. & Govorun, V. (2016) Agent Based Modeling of Human Gut Microbiome Interactions and Perturbations. *PLoS One*, **11**, e0148386. https://doi.org/10.1371/journal.pone.0148386.

Singh, P., Rawat, A., Alwakeel, M., Sharif, E. & Al Khodor, S. (2020) The potential role of vitamin D supplementation as a gut microbiota modifier in healthy individuals. *Sci. Rep.*, **10**,21641. https://doi.org/https://doi.org/10.1038/s41598-020-77806-4.

Smith, P. D., Smythies, L. E., Shen, R., Greenwell-Wild, T., Gliozzi, M. & Wahl, S. M. (2011) Intestinal macrophages and response to microbial encroachment. *Mucosal Immunol.*, **4**, 31–42. https://doi.org/10.1038/mi.2010.66.

Souberbielle, J. C., Massart, C., Brailly-Tabard, S., Cavalier, E. & Chanson, P. (2016) Prevalence and determinants of vitamin D deficiency in healthy French adults: the VARIETE study. *Endocrine*, **53**, 543–550. https://doi.org/10.1007/s12020-016-0960-3.

Stojanov, S., Berlec, A. & Štrukelj, B. (2020) The Influence of Probiotics on the Firmicutes/Bacteroidetes Ratio in the Treatment of Obesity and Inflammatory Bowel disease. *Microorganisms*, **8**. https://doi.org/10.3390/microorganisms8111715.

Stübler, S., Kloft, C. & Huisinga, W. (2023) Cell-level systems biology model to study inflammatory bowel diseases and their treatment options. *CPT Pharmacometrics Syst. Pharmacol*, **12**, 690–705. https://doi.org/10.1002/psp4.12932.

Tang, J. C. Y., Jackson, S., Walsh, N. P., Greeves, J., Fraser, W. D. & Bioanalytical Facility team (2019) The dynamic relationships between the active and catabolic vitamin D metabolites, their ratios, and associations with PTH. *Sci. Rep*, **9**, 6974. https://doi.org/10.1038/s41598-019-43462-6.

Tangestani, H., Boroujeni, H. K., Djafarian, K., Emamat, H. & Shab-Bidar, S. (2021) Vitamin D and The Gut Microbiota: a Narrative Literature Review. *Clin Nutr Res*, **10**, 181–191. https://doi.org/10.7762/cnr.2021.10.3.181.

Wu, Y. L., Xu, J., Rong, X. Y., Wang, F., Wang, H. J. & Zhao, C. (2021) Gut microbiota alterations and health status in aging adults: From correlation to causation. *Aging Med. (Milton)*, **4**, 206–213. https://doi.org/10.1002/agm2.12167.

Xong, X., Fu, J., Xu, B., Wang, Y. & Jin, M. (2020) Interplay between gut microbiota and antimicrobial peptides. *Anim Nutr*, **6**, 389–396. https://doi.org/10.1016/j.aninu.2020.09.002.

Yamamoto, E. A. & Jørgensen, T. N. (2020) Relationships Between Vitamin D, Gut Microbiome, and Systemic Autoimmunity. *Front. Immunol*, **10**, 3141. https://doi.org/10.3389/fimmu.2019.03141.

Zheng, D., Liwinski, T. & Elinav, E. (2020) Interaction between microbiota and immunity in health and disease. *Cell Res*, **30**, 492–506. https://doi.org/10.1038/s41422-020-0332-7.

Zhou, A., Yuan, Y., Yang, M., Huang, Y., Li, X., Li, S., Yang, S. & Tang, B. (2022) Crosstalk Between the Gut Microbiota and Epithelial Cells Under Physiological and Infectious Conditions. *Front. Cell. Infect. Microbiol*, **12**, 832672. https://doi.org/10.3389/fcimb.2022.832672.

Appendix A

Sensitivity of the full model to local changes in the baseline parameters given in Tables 2–5 is shown in Figs A31 (microbiota model parameters), A32 (vitamin D model parameters) and A33 (epithelial and immune response model parameters) for variables F, P, V_{D_a}, E and C.

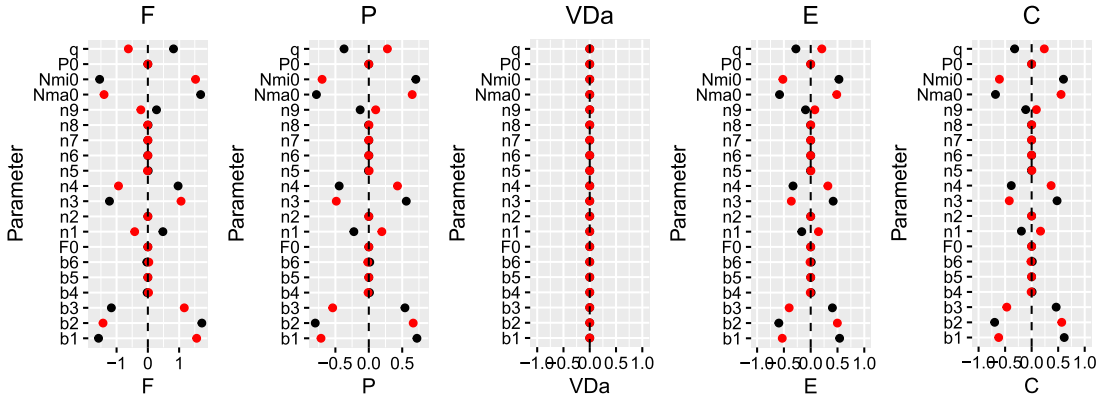

FIG. A31. The effect of varying parameter values on the steady state bacteria populations, VDR:1,25(OH)$_2$D complex, volume fraction of healthy epithelial cells and concentration of pro-inflammatory cytokines. Baseline parameter values are taken from Table 2 and each parameter is sequentially varied by a 10% decrease (black) and a 10% increase (red). Sensitivity is defined by equation (2.8). Note that n=η and b=β.

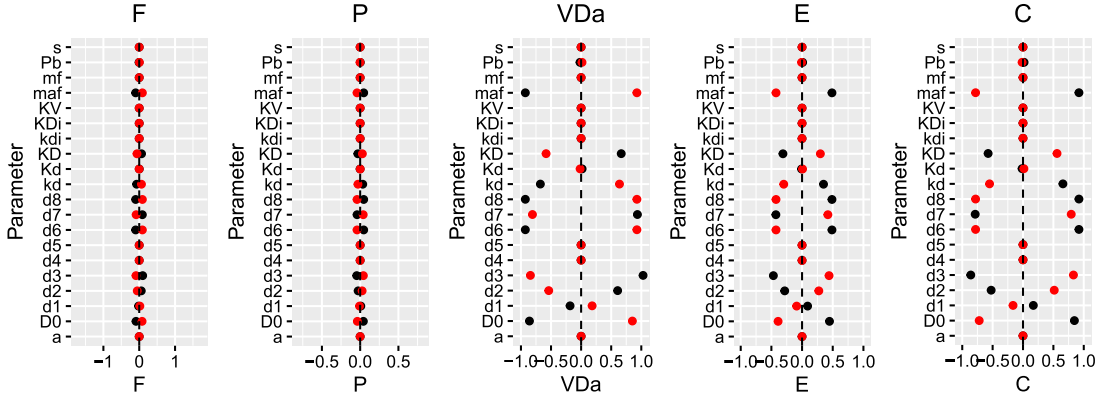

FIG. A32. The effect of varying parameter values on the steady state bacteria populations, VDR:1,25(OH)$_2$D complex, volume fraction of healthy epithelial cells and concentration of pro-inflammatory cytokines. Baseline parameter values are taken from Table 3 and each parameter is sequentially varied by a 10% decrease (black) and a 10% increase (red). Sensitivity is defined by equation (2.8). Note that m=μ, d=δ.

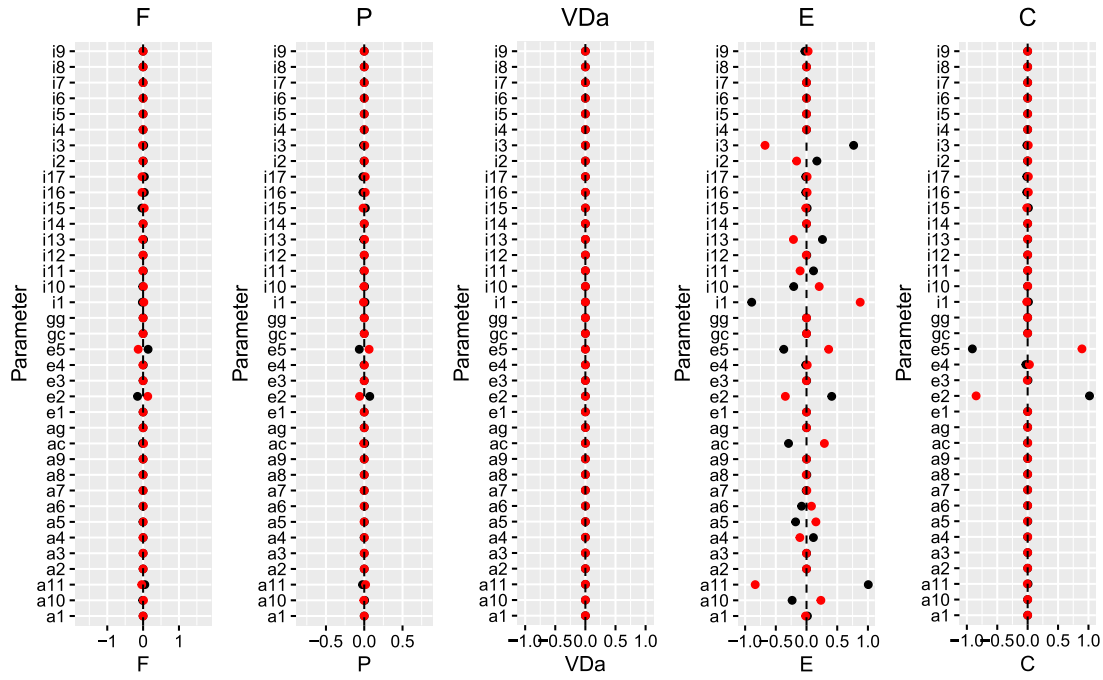

FIG. A33. The effect of varying parameter values on the steady state bacteria populations, VDR:1,25$(OH)_2$D complex, volume fraction of healthy epithelial cells and concentration of pro-inflammatory cytokines. Baseline parameter values are taken from Tables 4 and 5 and each parameter is sequentially varied by a 10% decrease (black) and a 10% increase (red). Sensitivity is defined by equation (2.8). Note that i=ι, a=α, e=ϵ and g=γ.